Geophys. J. Int. (2005) **163,** 813–832 doi: 10.1111/j.1365-246X.2005.02782.x

Late Jurassic–Early Cretaceous closure of the Mongol-Okhotsk Ocean demonstrated by new Mesozoic palaeomagnetic results from the Trans-Baïkal area (SE Siberia)

Jean-Pascal Cogné, Vadim A. Kravchinsky,* Nadir Halim and Fatim Hankard

Laboratoire de Paléomagnétisme, UMR CNRS 7577, *Institut de Physique du Globe & Université de Paris* 7, 4 *Place Jussieu,* F-75252 *Paris cedex* 05, *France. E-mail: cogne@ipgp.jussieu.fr*

Accepted 2005 August 9. Received 2005 July 20; in original form 2004 December 13

SUMMARY

We present new palaeomagnetic results from the Transbaïkal area (SE Siberia), from the Mongol-Okhotsk suture zone, the boundary between the Amuria and Siberia blocks. In order to better constrain the time of closure of the Mongol-Okhotsk Ocean in the Mesozoic, we collected 532 rock samples at 68 sites in six localities of basalts, trachy-basalts and andesites, from both sides of the Mongol-Okhotsk suture: at Unda river (J_3; 51.7°N, 117.4°E), Kremljevka peak (K_1; 51.8°N, 117.5°E) and Torey lakes (K_1; 50.1°N, 115.9°E) on the southern side of the suture, and at Monostoy river (J_1; 51.1°N, 106.8°E), Ingoda river (K_1; 51.2°N, 112.2°E) and Bichura town (K_1; 50.6°N, 107.6°E) on the northern side. Progressive thermal demagnetization enabled us to resolve low (LTC) and high (HTC) temperature components of magnetization at most sites. Jurassic palaeopoles computed from the HTCs show a large discrepancy with respect to the Apparent Polar Wander Path of Eurasia, which we interpret in terms of 1700–2700 km of post-Late Jurassic northward movement of Amuria with respect to Siberia. Although geological data suggest a middle Jurassic closure of the Mongol-Okhotsk Ocean in the west Trans-Baikal region, our data give evidence of a large remaining palaeolatitude difference between the Amuria and Siberia blocks. In contrast, Early Cretaceous sites cluster remarkably well along a small-circle, which is centred on the average site location. This implies the absence of post-Early Cretaceous northward motion of Amuria relative to Siberia, and demonstrates the pre-Early Cretaceous closure of the Mongol-Okhotsk Ocean. Finally, we interpret the very large tectonic rotations about local vertical axes, evidenced by the small-circle distribution of poles, as arising both from collision processes and from left-lateral shear movement along the suture zone, due to the eastward extrusion of Amuria under the effect of the collision of India into Asia.

Key words: Mongol-Okhotsk Ocean, palaeomagnetism, plate tectonics, Siberia.

1 INTRODUCTION

Among the numerous tectonic blocks that comprise the east of the Eurasia continent (Fig. 1), the history of the Amuria block, situated between Siberia to the north, and the North China (NCB), and Tarim (TAR) Blocks, to the south, is one of the less well constrained by palaeomagnetic data. This block is bounded to the north by the Mongol-Okhotsk fold belt, which stretches over 3000 km along the southwestern boundary of the Siberia craton from the Udsky Gulf of the Okhotsk Sea to Central Mongolia, through the eastern Trans-Baikal region, and to the south by the Gobi Altai mountain ranges, and the Gobi Desert. Zonenshain *et al.* (1990) argue that the Amuria microcontinent consists of a number of lithospheric blocks or terranes (Khangai, Khentei, Central Mongolian, Argun, Khingan-Bureya), which amalgamated in the Early Palaeozoic. All along the Trans-Baikal fold belt, which bounds the northern margin of the Amuria block, the occurrence of hyperbasites and ophiolites, as well as intrusions of gabbrotonalites and plagiogranites have lead several authors (e.g. Zonenshain *et al.* 1976; Kuzmin & Filippova 1979; Misnik & Shevchuk 1980; Parfenov 1984; Zonenshain *et al.* 1990; Nie 1991; Sorokin 1992) to propose that this fold belt is a suture zone between Siberia to the north and the Amuria (or Mongolia) block to the south. Radiometric dating of felsic intrusives along the suture shows progressively younger ages from west to east, with ages ranging from Late Carboniferous–Permian in Central Mongolia, to Triassic–Early Jurassic in western Transbaikalia,

*Now at: Physics Department, University of Alberta, Edmonton, AB, T6G 2J1, Canada.

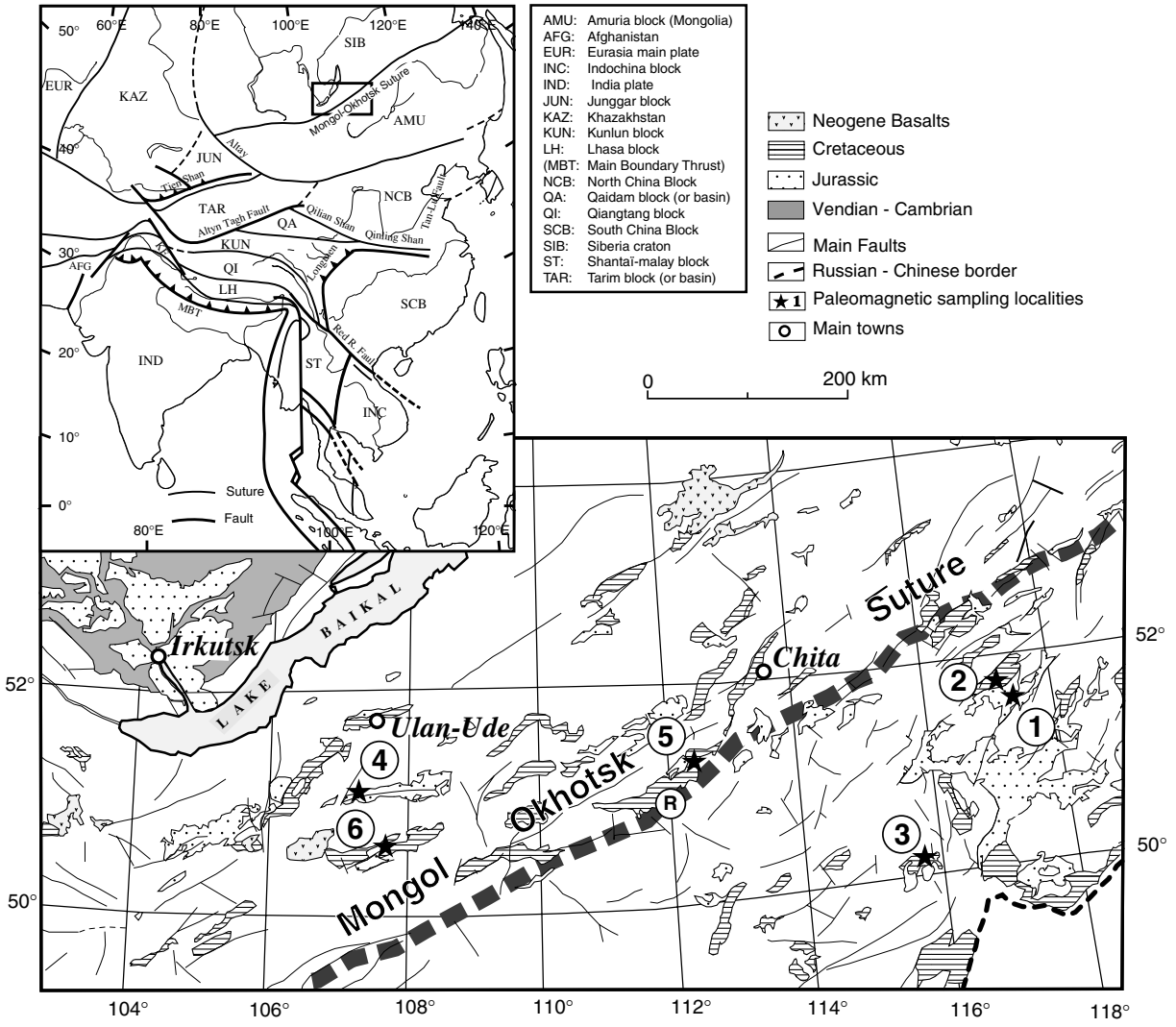

Figure 1. Top: Simplified map of southeast Asia showing the main sutures and faults bounding the different blocks. Bottom: simplified geological map of the southern border of the Siberian platform and the Western Trans-Baikal region (after Kravchinsky *et al.* 2002) with palaeomagnetic sampling localities of the present study (stars); bold grey hatched line: Mongol-Okhotsk geosuture. The localities are: (1)—Unda-Daya Depression (Tergen Formation, Late Jurassic); (2)—Kremljevka peak basalts (Early Cretaceous), (3)—Torey lakes basalts (Early Cretaceous), (4)—Monostoy Ridge basalts (Early Jurassic), (5)—Ingoda river basalts (Early Cretaceous), (6)—Bichura basalts (Early Cretaceous); the circled letter R is the reference point used in Table 3 and Fig. 10.

Late Jurassic in eastern Transbaikalia and Cretaceous in the Amur province, the far eastern part of south Siberia (Kuzmin 1985; Zonenshain & Kuzmin 1997). This eastward progression towards younger ages has been interpreted as a progressive, scissor-like, closure of the Mongol-Okhotsk Ocean separating these two landmasses. In this scheme, the collision of Amuria with Siberia began at the end of the Carboniferous in the west and terminated in the east at the beginning of the Cretaceous.

Existing palaeomagnetic studies in this region are quite scarce, but they do not contradict this idea. Geological and palaeomagnetic evidence (Pruner 1992) show that Amuria and the NCB were accreted together by the Late Carboniferous. Xu *et al.* (1997) noted a large palaeolatitude discrepancy between Amuria and Siberia in the Permian. Kravchinsky *et al.* (2002) reappraised the data of Xu *et al.* (1997), which come from the Chita region, south of the suture, and reach similar conclusion. Palaeomagnetic data from the NCB and South China Block (SCB; Lin *et al.* 1985; Zhao Coe 1987; Huang & Opdyke 1991; Enkin *et al.* 1991, 1992; Yang *et al.* 1992; Gilder *et al.* 1993, 1996; Gilder & Courtillot 1997; Yang & Besse 2001) are consistent with this model. They show that the continental landmass composed of Amuria, NCB and SCB was not accreted to Siberia before the Cretaceous, implying a large oceanic gap (the Mongol-Okhotsk Ocean) between Amuria and Siberia before that time. A preliminary palaeomagnetic study of Cretaceous volcanics from the Amur province (Halim *et al.* 1998a) appears to confirm that the Mongol-Okhotsk Ocean had closed by the Early Cretaceous. Finally, apart from the first results of Kravchinsky (1995) and Kuzmin & Kravchinsky (1996), published in Russian, and the more recent study of Kravchinsky *et al.* (2002), few detailed palaeomagnetic results are yet available from within the suture zone itself. In particular, no Early Cretaceous palaeomagnetic results have ever been published from the southern Siberian and northern Amurian regions.

In order to complement data from Kravchinsky *et al.* (2002), which only constrain the history of Mongol-Okhotsk geosuture prior to the Late Jurassic, and those from Halim *et al.* (1998a), we present here new results of a palaeomagnetic investigation of samples from

six Early Jurassic to Early Cretaceous localities situated on both sides of the Mongol-Okhotsk suture zone.

2 SAMPLING AND PALAEOMAGNETIC ANALYSIS

In order to constrain the past large-scale motions that have occurred between Amuria and Siberia, we have carried out during the summer 1997, in the framework of a Franco–Russian cooperation programme, a field trip along the Mongol-Okhotsk suture in the Trans-Baikal area of Siberia, during which Jurassic and Early Cretaceous volcanics were sampled. During this field trip, we collected 532 cores at 68 sites in six localities from both sides of the suture (Table 1, Fig. 1). In general, eight cores were drilled at each site using a gasoline-powered drill, and oriented *in situ* using magnetic and, whenever possible, sun compasses, in order to check and correct orientations for local magnetic field declination.

A summary of this collection is given in Table 1. All the localities which are basalts, trachy-basalts and trachy-andesites have been dated, either by stratigraphy (e.g. localities 1, 3 and 6), and/or using radiometric methods (localities 2, 3, 4 and 5). In general, magnetic field declinations we measured in the field are in good agreement with the declination computed for summer 1997 from the IGRF 1995 coefficients and their time derivatives. A noticeable exception is the Kremljevka peak locality (locality 2) where very high intensities of natural remanent magnetization (NRM), which are probably due to lightning strikes on the outcrop, as discussed below, probably disturb magnetic compass readings. Whenever possible, measured declinations were used to correct field magnetic azimuths, otherwise (sites 1, 2, 3), we used the IGRF declination of -9.0° at that place.

Standard cores of 2.5 cm diameter were cut into 2.3-cm-long specimens in the palaeomagnetic laboratory of the Institut de Physique du Globe de Paris (IPGP)/Université de Paris 7. All the magnetic measurements were performed in a magnetically shielded room. Remanent magnetizations were measured using a 2G enterprises three-axis cryogenic magnetometer. Specimens from the Kremljevka peak locality were measured on a JR-5 spinner magnetometer, due to their high NRM intensities. Specimens were thermally demagnetized up to 580°C or 685°C. Acquisition of isothermal remanent magnetization (IRM) experiments were performed in order to help identify the magnetic minerals. Palaeomagnetic directions at the specimen level were determined using principal component analysis (Kirschvink 1980). Site-mean and overall mean directions were computed using Fisher (1953) statistics. All the interpretations and data processing have been done using the *PaleoMac* software package we developed at IPGP (Cogné 2003).

3 RESULTS

3.1 Amuria block

3.1.1 Late Jurassic Tergen Formation—Unda river locality

From the 12 sites sampled in the Late Jurassic (J_3) Tergen Formation, 5 sites (13–17) were taken in basalt flows, and 7 sites (18–24) in interbedded trachy-andesites. A difference exists between these two groups regarding NRM intensities, which are of the order of 0.1–1 A m^{-1} for the basalts, and 0.01–0.1 A m^{-1} for the trachy-andesites. Thermal demagnetizations (Figs 2a and b) isolated a low-temperature component (LTC) between NRM and 300°–400°C in most specimens. This LTC, which is well defined in 10 out of the

Table 1. Summary of palaeomagnetic sampling of Jurassic and Cretaceous effusives from the Mongol-Okhotsk Suture zone.

Locality	Lat/Long	Formation	Rock type	Age	Method	Reference	Sites Id	N/n	Dec	D_{IGRF}
South of the Mongol-Okhotsk suture—Amuria block										
1. Unda river ([1])	51.7°N/117.4°E	Tergen	basalts and trachy-andesites	J_3	Stratigraphic	Skoblo & Lyamina (1985) Sinitsa & Starukhina (1986)	13–24	12/91	$-8.8^\circ \pm 0.9^\circ$ ($n = 52$)	-9.0°
2. Kremljevka Peak	51.8°N/117.5°E	Kremljevka	basalts	125–133 Ma	Ar/Ar	Shubkin *et al.* (1992)	01–12	12/98	scattered	-9.0°
3. Torey lakes ([2])	50.1°N/115.9°E	Torey	basalts	~120 Ma	K/Ar	Cherbanova & Zvonkova (1966)	25–38	14/108	$-9.1^\circ \pm 0.9^\circ$ ($n = 38$)	-8.0°
				K_1	Stratigraphic	Skoblo & Lyamina (1985) Srebrodol'skaya (1984)				
North of the Mongol-Okhotsk suture—Siberia block										
4. Monostoy river	51.1°N/106.8°E	Monostoy	basalts and trachy-basalts	188 Ma	Rb–Sr	Yarmoljuk *et al.* (2000)	61-68	8/61	$-4.4^\circ \pm 2.3^\circ$ ($n = 27$)	-3.7°
5. Ingoda river	51.2°N/112.2°E	Ingoda	trachy-basalts	118–128 Ma	K/Ar	Kazimirovsky & Drill (1991) Kazimirovsky (1994)	39–50	12/93	$-8.9^\circ \pm 2.5^\circ$ ($n = 48$)	-6.5°
6. Bichura	50.6°N/107.6°E	Bichura	basalts and trachy-basalts	K_1	Stratigraphic	Skoblo & Lyamina (1985)	51-60	10/81	$-3.0^\circ \pm 0.8^\circ$ ($n = 8$)	-4.0°

Lat/Long: average Latitude and Longitude of the sampling sites; *N/n* Number of sites/number of cores; December: local magnetic field declination computed after magnetic and sun compasses readings, D_{IGRF}: local magnetic field declination computed for the summer 1997, after the IGRF coefficients of 1995 and their time derivatives; Notes: ([1]) The Tergen Formation overlies the J_{2-3} Shadaron Formation, which has been palaeomagnetically studied by Kravchinsky *et al.* (2002); ([2]) two groups of flows (29–35 and 25–28 plus 36–38) separated by 1 km; the lateral relationships between these different stacks of flows is difficult to assess.

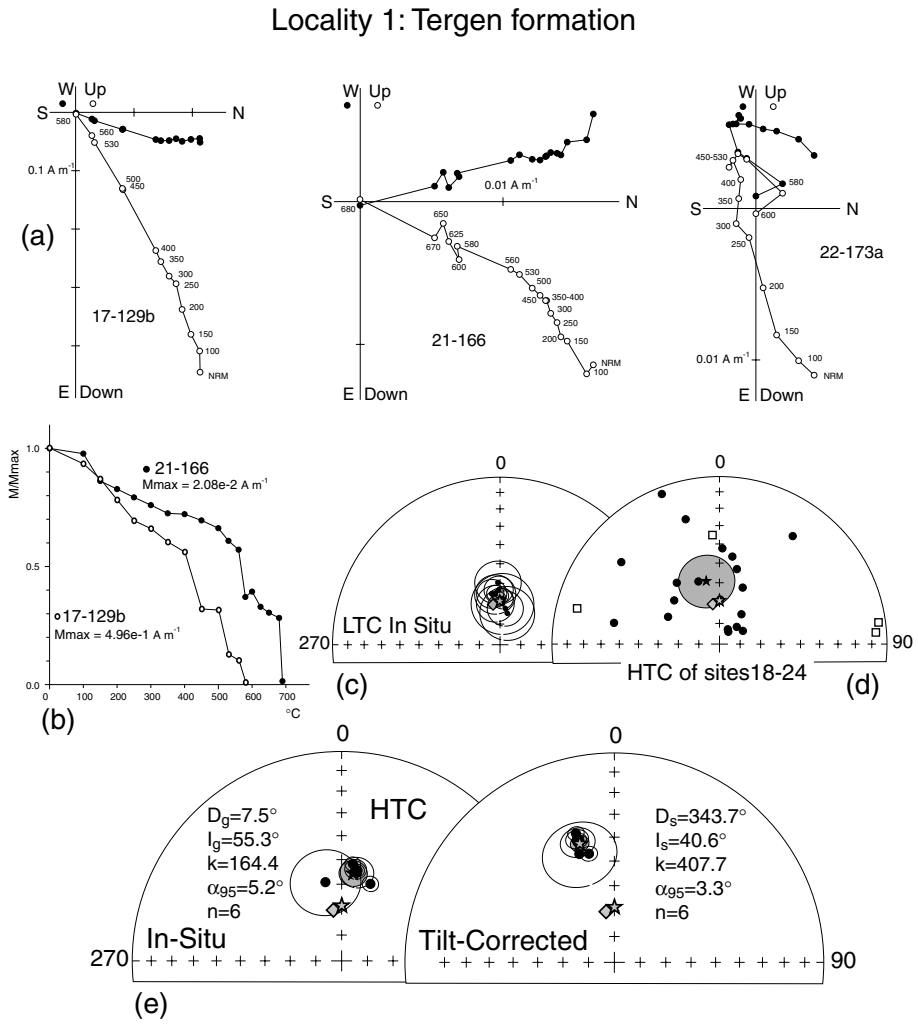

Figure 2. Results of thermal demagnetization of Unda river locality samples of the Tergen Formation. (a) orthogonal vector plots of thermal demagnetizations (*in situ* coordinates), of basalt and andesites samples; closed (open) symbols: projection onto the horizontal (vertical) plane; temperatures are indicated in °C. (b) magnetization decay curves (c) Equal-area projection of *in situ* LTC site mean directions with their α_{95} circles of confidence. (d) Equal-area projection of specimen *in situ* HTC of samples from sites 18–24; white squares are data excluded from the average. (e) Equal-area projections of site-mean HTC of sites 13–17 and average site 18–24 shown as *in situ* (left) and tilt-corrected (right). Black stars with grey α_{95} areas in (c) (d) and (e) are the overall means; grey star: dipole field direction, grey diamond IGRF direction; closed (open) symbols: positive, downwards, (negative, upwards) inclinations.

12 sites, averages at (Fig. 2c): $D_g = 359.0°$, $I_g = 67.3°$ ($k_g = 248.3$, $\alpha_{95} = 3.1°$) and $D_s = 336.6°, I_s = 51.4°$ ($k_s = 52.4, \alpha_{95} = 6.7°$), $n = 10$ sites, in geographic and stratigraphic coordinates, respectively. With a ratio $k_g/k_s = 4.738$, the fold test (McElhinny 1964) is negative at the 99 per cent probability level, and the *in situ* average direction of LTC conforms to the present-day geocentric axial dipole (GAD) field direction ($D = 0°$, $I = 68.7°$). Therefore, the LTC is interpreted as a recent magnetization, of either viscous or weathering origin.

After removal of this LTC, the behaviour of magnetization is drastically different between specimens taken from basalts and those coming from andesites. In the first case (sites 13–17; Figs 2a and b and Table 2), a well-defined high-temperature component (HTC) directed downward in a northerly direction and converging toward the origin of orthogonal vector plots (Zijderveld 1967) is isolated between 400°C and 580°C. This maximum unblocking temperature indicates that the HTC is carried by magnetite. For these basalt flows, the HTC shows a very good cluster both within and between sites (Fig. 2e; Table 2).

Samples of andesites (sites 18–24) show different and less well-behaved demagnetization paths. As shown by specimen 21–166 (Figs 2a and b), NRM partly demagnetizes between 400°C and 580°C, then stabilizes between 580°C and 650–670°C and falls rapidly to zero at 680°C. This indicates the presence of haematite. Furthermore, due to the very low intensity of magnetization in these samples, the later demagnetization steps were often noisy (specimen 22-173a, Fig. 2a), probably because of spurious magnetizations due to thermal alteration of the samples during the experiments. In this group of sites, the HTC could be resolved in only 23 out of the 44 specimens demagnetized. Note that the magnetization of specimen 22-173a in Fig. 2(a) evolves toward a southerly upward direction, which is quite rare, most of the samples of sites 18–24 giving normal, albeit scattered, north and downward HTC. Because it was impossible to define a within-site mean direction at all of the sites 18–24, and because of large scatter of individual HTC of these andesites, as illustrated in Fig. 2(d), we computed a single average of all the specimen HTC that could be resolved in these sites. As may be seen in Fig. 2(d), 4 out of the

Table 2. Site-mean palaeomagnetic direction for the high-temperature component of Jurassic and Cretaceous effusives from the Mongol-Okhotsk Suture zone.

Site	Strike/Dip	*n*/*N*	*Dg*	*Ig*	*Ds*	*Is*	*k*	a_{95}	
1. J_3 Tergen Formation—Unda river locality (51.7°N, 117.4°E)									
13	207/28	5/7	9.9	54.7	343	39.9	153.4	6.2	
14	207/28	6/7	10	53.9	344.1	38.9	704.8	2.5	
15	207/28	6/7	6.6	51.5	343.4	35.9	540	2.9	
16	207/28	7/7	8.7	53.5	343.1	38.5	225.5	4	
17	207/28	7/9	20.5	57.8	346.8	45.7	280.3	3.1	
Sites 18–24	246/15	19/23	348.4	58.5	—	—	7.4	13.2	
(see text)			—	—	342.1	44.8	7.1	13.5	
average HTC		6/6	7.5	55.3	—	—	164.4	5.2	
		—	—		343.7	40.6	407.7	3.3	
2. K_1 Kremljevka peak locality (51.8°N, 117.5°E)									
01	58/13	7/7	331.5	54.2	333.2	67.2	106.8	5.9	
02	131/17	6/7	2.6	58.9	334.0	69.6	132.0	5.9	
03	33/16	3/7	331.6	59.8	355.2	72.3	628.9	4.9	
04	76/16	6/7	350.0	63.5	355.4	79.4	137.4	5.7	
05	99/14	7/7	4.5	65.1	359.0	79.0	229.8	4.0	
06	variable	6/7	359.1	61.7	—	—	414.7	3.3	
06		—	—	353.5	64.7	305.3	3.8		
07	157/7	5/7	0.2	72.2	337.7	73.7	49.7	11.0	
08	143/4.5	3/7	13.4	58.0	8.2	61.3	448.0	5.8	
09	264/3.5	7/7	27.4	70.9	22.6	67.9	607.0	2.5	
10	245/3.5	7/7	6.1	59.4	3.3	56.3	552.3	2.6	
11	0/0	7/7	8.8	70.3	8.8	70.3	366.3	3.2	
12	0/0	7/7	346.8	67.6	346.8	67.6	1491.9	1.6	
Average HTC		12/12	357.1	64.3	—	—	75.9	5.0	
		—	—		355.6	69.7	89.6	4.6	
3. K_1 Torey lakes locality (50.1°N, 115.9°E)									
25	23/15	7/7	107.6	−34.7	106.1	−49.6	68.5	7.9	3*d*+4*gc*
26[1]	*21/15*	*5/6*	*189.9*	*18.0*	*185.7*	*14.4*	*274.2*	*4.6*	*5gc*
27	21/15	6/7	122.3	−25.6	124.3	−40.2	159.1	5.6	4*d*+2*gc*
28	21/15	5/7	126.8	−31.6	130.7	−46.9	42.2	11.9	5*d*
29	0/0	6/6	181.2	−58.3	181.2	−58.3	472.5	3.1	6*d*
30	0/0	8/8	167.2	−62.9	167.2	−62.9	377.4	2.9	8d
31	0/0	5/5	168.8	−54.9	168.8	−54.9	527.8	3.3	5*d*
32	0/0	6/6	170.6	−54.7	170.6	−54.7	622.4	2.7	6*d*
33	0/0	3/4	162.0	−43.2	162.0	−43.2	1197.7	5.9	3*d*
34	0/0	4/4	172.3	−48.8	172.3	−48.8	470.4	4.2	4*d*
35[2]	0/0	1/4			1 pole to great-circle: $D = 242.6°$, $I = 13.5°$				
36	18/15	6/6	119.6	−35.1	122.7	−49.7	118.5	6.2	6*d*
37	18/15	4/4	324.6	41.1	335.3	52.3	22.0	23.2	2*d*+2*gc*
38	18/15	5/6	114.5	−43.7	117.0	−58.6	98.1	8.8	2*d*+3*gc*
HTC Averages									
Group 1 ‘	(sites 29 to 34)	6/7	170.0	−54.0	170.0	−54.0	104.9	6.6	
Group 2[3]	(25–28 and 36–38)	7/7	121.3	−36.3	—	—	48.3	8.9	6*d*+1*gc*
		—	—		125.9	−50.5	47.7	8.9	
Mean Inclination		12/14	—	−44.5	—	—	24.2	8.9	
		—	—		—	-51.7	75.1	5.0	
All HTC[4]		12/14	350.0	44.6	—	—	33.7	7.8	
(Normal polarity)			—	—	350.0	51.8	94.9	4.6	
4. J_1 Monostoy locality (51.1°N, 106.8°E)									
61	28/46	5/5	311.9	46.4	47.5	80.3	6.6	32.1	
62	42/45	5/6	330.3	44.2	47.1	77.1	335.3	4.2	
63	37/33	5/7	334.6	77.9	113.0	67.2	39.7	12.3	
64	87/52	10/10	137.8	−30.3	87.9	−56.6	34.0	8.4	
66	47/34	9/9	301.7	58.1	203.8	81.2	16.9	12.9	
67	39/32	8/8	303.9	73.4	135.3	74.5	36.5	9.3	
68	5/58	6/9	287.0	71.4	89.6	49.6	777.1	2.4	
Average HTC[5]		5/7	316.1	60.6	—	—	23.4	16.1	
		5/7	—	—	105.6	80.6	40.0	12.2	

23 HTC (white squares) show anomalous directions with negative inclinations in north, west and east directions. These four specimens have been excluded from the mean displayed in Table 2. This overall mean, computed at the specimen level for sites 18–24, is assumed to characterize the poorly defined average HTC of andesites, and is given the same weight as each of the basalt sites 13–17 in the computation of the final average of Tergen Formation magnetization.

Table 2. (*Continued.*)

Site	Strike/Dip	*n*/*N*	*Dg*	*Ig*	*Ds*	*Is*	*k*	a_{95}	
5. K_1 Ingoda river locality (51.2°N, 112.3°E)									
39	—	5/6	51.2	72.0	51.2	72.0	299.4	4.4	
40	—	6/6	52.9	73.4	52.9	73.5	533.0	2.9	
41	—	6/6	37.3	73.3	37.3	73.3	88.9	7.1	
42	—	7/7	49.5	73.7	49.5	73.7	480.9	2.8	
43	—	5/5	32.8	74.2	32.8	74.2	638.1	3.0	
44	—	5/5	27.9	65.2	27.9	65.2	74.7	8.9	
45	—	6/6	66.4	66.1	66.4	66.1	591.2	2.8	
46	—	6/6	73.5	65.7	73.5	65.7	238.4	4.3	
47	—	5/6	63.3	65.9	63.3	65.9	409.4	3.8	
48	—	6/6	64.1	66.5	64.1	66.5	95.7	6.9	
49	—	6/6	64.0	70.5	64.0	70.5	52.2	9.4	
50	—	6/6	41.5	64.0	41.5	64.0	103.5	6.6	
Average HTC	—	12/12	52.8	69.8	52.8	69.8	150.5	3.5	
6. K_1 Bichura locality (50.6°N, 107.6°E)									
51[(6)]	205/11.5	4/7	79.9	−10.4	80.6	−1.0	79.0	10.4	
52	205/11.5	5/5	17.2	−83.5	83.6	−77.6	21.7	19.0	2*d*+3*gc*
53	205/11.5	5/8	25.4	78.8	340.0	74.1	93.3	8.0	
54	192/7.5	7/7	43.8	−60.0	53.4	−55.6	22.3	13.9	3*d*+4*gc*
55	192/7.5	7/7	23.8	−78.7	53.2	−75.3	113.4	5.7	
56	192/7.5	6/6	28.0	−69.5	44.9	−66.3	282.1	4.0	
57	250/45	7/7	351.8	−49.8	105	−80.7	211.5	4.2	
58	250/45	6/6	355.2	−48.7	95.0	−79.0	114.1	6.3	
59	250/45	7/8	25.8	−34.6	69.6	−53.9	41.2	9.5	
60	3/21	4/5	108.6	−56.5	129.9	−75.7	752.5	3.6	3*d*+1*gc*
Average HTC	—	9/10	205.7	69.1	—	—	10.2	16.9	
			—	—	257.3	74.1	29.2	9.7	

Strike/dip: strike and dip (in the Strike+90° direction) of the flow planes; *n*/*N*: at the site level: number of entries in the statistics/number of demagnetized specimens; at the formation level: number of entries in the statistics/number of sites; *Dg*, *Ig* (*Ds*, *Is*): declination, inclination in geographic (stratigraphic) coordinates; *k*, a95: Fisher (1953) statistics parameters; *d*, *gc*: number of vectors, number of great-circles used in mixed average computations. Notes: ([1]) Site 26: normal to mean remagnetization great-circles; ([2]) Site 35: only one remagnetization great-circle; excluded from computations; ([3]) Group 2 average including Site 26; ([4]) formation average excluding Site 26; ([5]) Monostoy average excluding sites 64 and 68; ([6]) Site 51 excluded from the formation mean.

The final mean for the Late Jurassic Tergen Formation is: $D_g = 7.5°$, $I_g = 55.3°$ ($k_g = 164.4, \alpha_{95} = 5.2°$) *in situ*, and $D_s = 343.7°$, $I_s = 40.6°$ ($k_s = 407.7, \alpha_{95} = 3.3°$), $n = 6$ after tilt correction (Fig. 2e, Table 2). Although the population appears to cluster upon untilting, the k_s/k_g value of 2.480, compared to the *F* statistics of 2.970 and 4.850 at the 95 and 99 per cent probability levels, indicates an inconclusive fold test, following either McElhinny (1964) or McFadden (1990). This is not surprising, considering the small angle between the tilt of the different sites, and the fact that the increase in *k* parameter is mainly due to one poorly defined average (sites 18–24 mean) joining the group of sites 13–17. However, because neither *in situ* nor tilt-corrected (TC) populations contain the present-day dipole field direction, and although most of the sample display normal polarity directions, with almost no reverse ones, we assume that the tilt-corrected HTC average is the characteristic remanent magnetization of Late Jurassic age for this formation.

3.1.2 Kremljevka Formation Early Cretaceous basalts

Although IRM acquisition curves (Fig. 3a) provide evidence for a single low-coercivity magnetic carrier, thermal decay of magnetization (Fig. 3b, specimen 07–51) clearly shows two unblocking temperature ranges, one at 350°–400°C, followed by a higher one around 580°C. Although the temperature spectra appear to be well separated on magnetization decay curves, simple thermal stepwise demagnetization appeared inefficient in separating multicomponent magnetizations (e.g. Fig. 3c, spec. 07–51). We thus adopted a composite demagnetization procedure, where the low-coercivity, low-temperature magnetic carrier was demagnetized first using two thermal demagnetization steps, up to 200°C, followed by a few steps in alternating field (AF) demagnetization up to 60 mT. Complete demagnetization is then achieved by thermal demagnetization from 300°C to 580°C. (Fig. 3b, spec. 02-17b). This allowed us to remove a strong magnetic component (Fig. 3d), representing 30–95 per cent of the total NRM intensity, and responsible for the abnormally high NRM intensity values (often ranging 100–200 A m^{-1}) characteristic for the samples of this locality. This low-coercivity, LTC has been resolved in 53 specimens, and is shown in Fig. 3(e), where it appears to be completely inconsistent, except for a tendency to show low-to-intermediate inclinations. Altogether, these observations (low coercivity, high intensity, large scatter) lead us to interpret this component as probably being an IRM due to lightning strikes.

After removing of this LTC, composite demagnetization treatment allowed us to isolate a stable, HTC magnetization between 400°C and 580°C at each site (Figs 3d and f: Table 2). Although it was difficult to resolve in some sites (e.g. sites 3 and 8, Table 2), because of the strong IRM overprint, it is generally well defined. The HTC shows systematic north downward directions (Fig. 3f) and averages as $D_g = 357.1°$, $I_g = 64.3°$ ($k_g = 75.9, \alpha_{95} = 5.0°$) and $D_s = 355.6°$, $I_s = 69.7°$ ($k_s = 89.6, \alpha_{95} = 4.6°$), $n = 12$ sites, in geographic and stratigraphic coordinates, respectively. Although the HTC population tends to cluster upon untilting, the k_s/k_g ratio

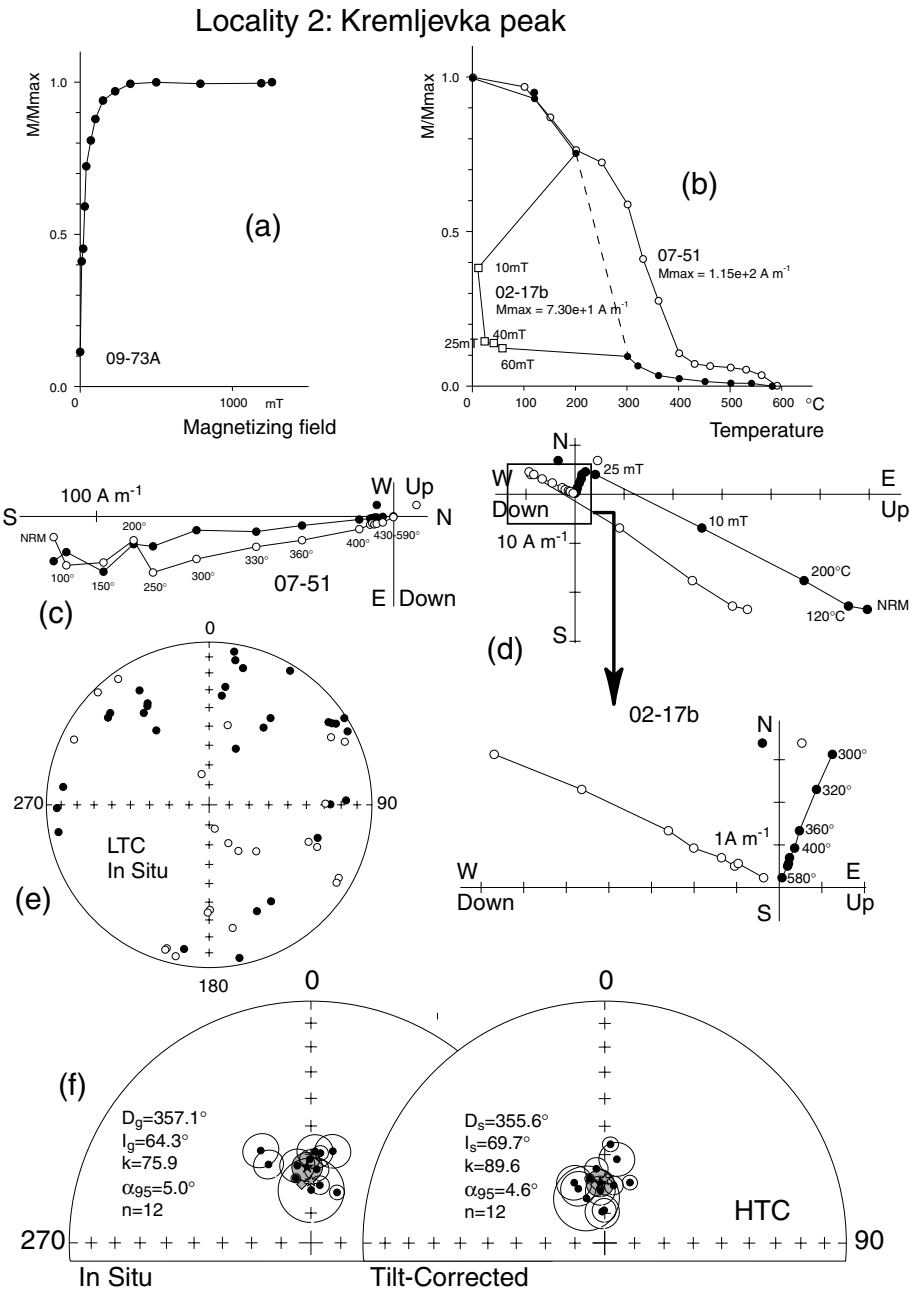

Figure 3. Results from Kremljevka Peak samples. (a) Isothermal remanent magnetization (IRM) acquisition curve in fields up to 1.2 T displaying a saturation by ∼0.3 T. (b) Magnetization decay curve during thermal demagnetization (specimen 07-51, white circles) and in composite AF (white squares) and thermal (black dots) demagnetization (specimen 02-17b). (c) Orthogonal vector plot (*in situ* coordinates) of specimen 07-51 thermal demagnetization. (d) Orthogonal vector plots, of specimen 02-17b composite demagnetization. Temperatures are indicated in °C and AF values in mT. (e) Equal-area *in situ* projection of specimen LTC. (f) Equal-area projections of HTC site-mean directions with their α_{95} cones of confidence before and after tilt correction. Black stars and shaded α_{95} areas in (f) indicate the overall mean HTC directions; grey star: dipole field direction, grey diamond IGRF direction; closed and open symbols in (c, d, e and f) as in Fig. 2.

of 1.180 indicates an inconclusive fold test, which is due to the low tilt of the flows. We finally note that the *in situ* average does not contain the present-day IGRF or dipolar field directions, but that the TC one does. This curious situation will be discussed below.

3.1.3 Early Cretaceous Torey Formation basalts

We sampled two outcropping flow stacks, separated by 1 km, one made of seven superposed flows (sites 29–35), the other one including superposed flows 25–28 and 36–38. Thermal demagnetization of the basalts of the Torey lakes locality (Fig. 4) reveals two magnetization components, although IRM acquisition curves (Fig. 4a) suggest a single, low-coercivity, magnetic phase. A first, LTC demagnetizes between NRM and 300°–400°C. The relative contribution of LTC to the total NRM is variable, ranging from a few percent (e.g. specimen 29–223, Fig. 4b) to more than 90 per cent (specimen 27-208, Fig. 4c). There is no clear relationship between the LTC percentage and the NRM intensity, which averages 0.630 ± 0.570 A m^{-1}

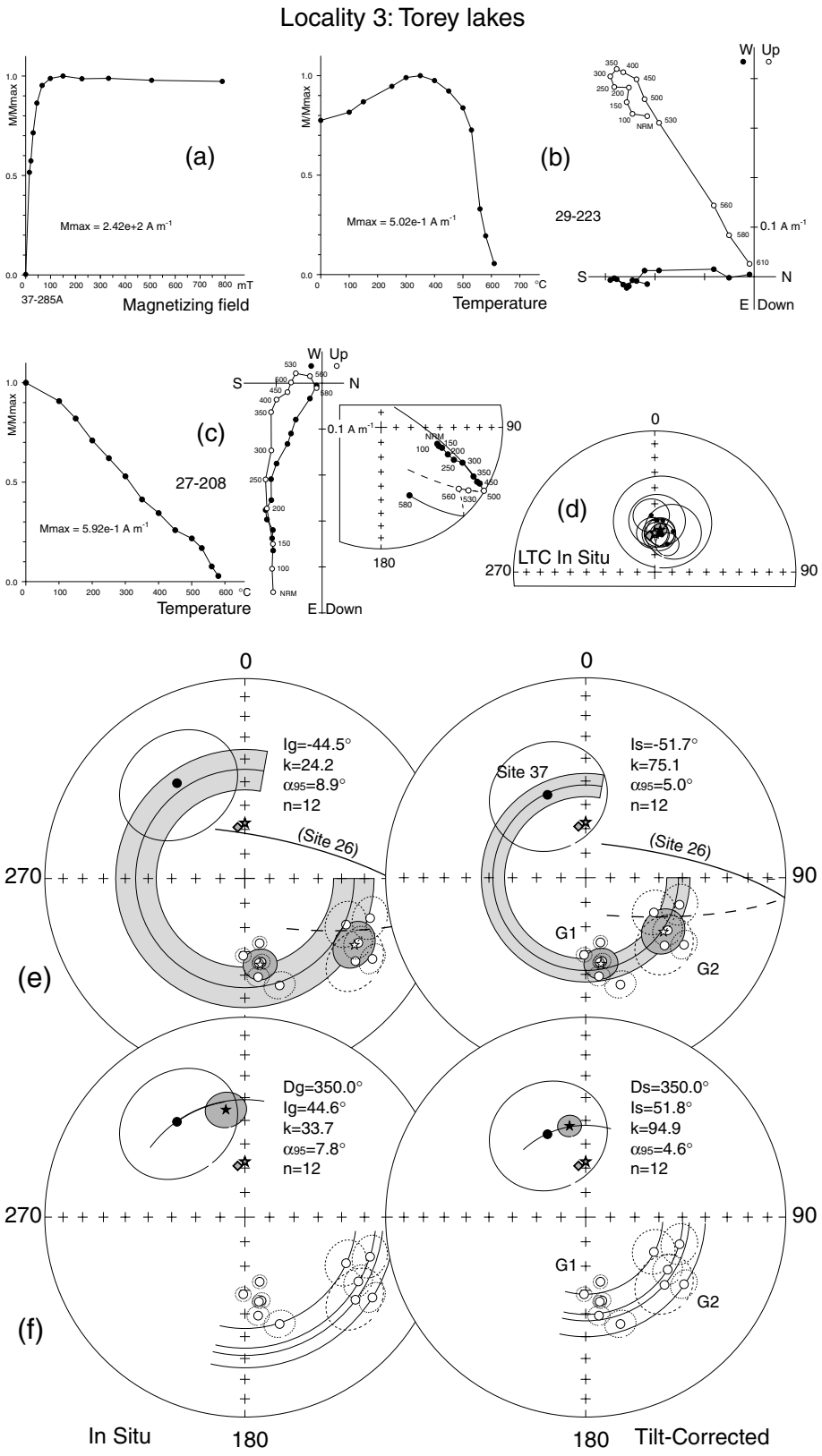

Figure 4. Results from Torey Lakes samples. (a) Isothermal remanent magnetization (IRM) acquisition curve in fields up to 0.8 T. (b, c) Thermal demagnetization shown as magnetization decay curves, *in situ* orthogonal vector plots and *in situ* equal-area projections for various cases of magnetization behaviour (see text). Temperatures are indicated in °C. (d) Equal area *in situ* projection of site-mean LTC directions. (e,f) Equal area-projections of site-mean HTC shown *in situ* (left) and tilt-corrected (right); G1 and G2 refer to Group 1 and Group 2 sites (see text and Table 1); light grey areas in (e) are the circles of mean inclination (McFadden & Reid 1982); curves in (f) are constant inclination circles passing through Group 2 site-mean directions; other conventions in (b)–(f) as in Fig. 2.

($n = 81$), but the group of flows 29–35 generally shows a weak LTC, except site 35 where it prevails, whereas the other sites show fairly high to predominant LTC. This component has been resolved in 10 out of the 14 sampled flows and it averages at: $D_g = 7.5^\circ$, $I_g = 65.4^\circ$ ($k_g = 166.9, \alpha_{95} = 3.8^\circ$), $n = 10$ in *in situ* coordinates (Fig. 4d). The k parameter decreases from 166.9 to 120.0 upon untilting, which is not significant at the 95 per cent probability level, mainly because of the very small dips of the flows (Table 2). However, the *in situ* average contains the present-day GAD field direction ($D = 0^\circ$, $I = 67.3^\circ$), and is therefore assumed to be a recent overprint.

After removal of this LTC, thermal demagnetization reveals a HTC, which generally unblocks between 500°C and 560°C, with a few samples yielding a slightly higher unblocking temperatures of 610°–630°C (e.g. specimen 29–223, Fig. 4b). Indeed, we find again that this component may be easily defined in specimen from flows 29 to 34 (specimen 29–223, Fig. 4b) where the LTC is weak, and with more difficulty in the other sites. In effect, because of the weak intensity of the HTC, demagnetization trajectories very seldom converges towards the origin (e.g. specimen 27-208, Fig. 4c). In that case, we have used the remagnetization circle method (Halls 1978), and computed the within-site means (Table 2) using the combined average of vectors and planes of McFadden & McElhinny (1988).

Except for only two specimens from site 37, the HTC shows systematic south to southeast upward directions (Table 1), or, in the case where HTC could not be isolated, the remagnetization circles (Fig. 4c) systematically evolve from the north downward direction of LTC toward south and upward directions. Consistent within-site mean HTC directions (Table 1, Fig. 4e) could be computed at every site except 35 and 26. At site 35, only one remagnetization great-circle could be determined, other specimens providing a north and downward magnetization, conforming to the present-day dipole field direction. Consequently, this site was excluded from all average computations that follow. In site 26, however, we could compute an average remagnetization great-circle from five out of the six demagnetized specimens.

Here again, we find a difference between the two sampled outcrops (Fig. 4e). Whereas the flows 29–34 (Group 1) show high within-site cluster and south upward directions, the second group (except site 37) show less well-defined within-site means, and southeasterly declinations. This larger scatter at the site level for the Group 2 data probably arises from the poor separation of LTC and HTC, leading us to compute site means using mixed statistics of vectors and great-circles, as mentioned above. One could evoke the same cause for the southeast declinations of this group. In effect, a poor separation of HTC from LTC could deflect the average toward the east, on the great-circle joining the HTC to the LTC. However, in sites 28 and 36 pertaining to this group, the averages have been obtained from HTC clearly converging to the origin of the Zijderveld plots, and it seems unlikely that there is a total overlapping of LTC and HTC unblocking temperature spectra, at least in these two sites.

We have computed an average for each group of flows (Table 1, Fig. 4e). The mean of Group 2 includes the average great-circle of site 26. Because the flows of Group 1 are flat lying, and those from the Group 2 have very similar tilts, none of these averages allows a fold test. However, one may note that untilting produces a clustering in inclinations between the two groups. In effect, the difference in inclination between the two means is $18.2^\circ \pm 12.0^\circ$ before, and $3.5^\circ \pm 12.0^\circ$ after tilt correction. This feature is also evidenced by the computation of the average inclination for all the data (excluding site 26 mean great-circle), following the statistics of McFadden & Reid (1982), which averages as $I_g = -44.5^\circ$, $k_g = 24.2, \alpha_{95} = 8.9^\circ$ *in situ*, and $I_s = -51.7^\circ$, $k_s = 75.1, \alpha_{95} = 5.0^\circ$, $n = 12$ after tilt correction (see small circles in Fig. 4e). The k_s/k_g ratio of 3.103 is above the F statistics of 2.050 and 2.816 at the 95 and 99 per cent probability levels. Although not very strong, this indicates a positive inclination-only test, and we therefore assume that HTC are indeed the primary magnetization of these basalts.

Although the above analysis of inclinations is sufficient to confidently determine a palaeolatitude for Torey lakes basalts, we attempted to compute a single average for all the sites, making the assumption that the difference in declination between the two groups arises from a relative rotation of the sampled outcrops around a vertical axis. Arbitrarily taking the Group 1 HTC directions as a fixed reference, we have computed a mixed average between these HTC and small-circles passing through the HTC site mean directions of Group 2. This average is an extension of the combined statistics of McFadden & McElhinny (1988) to the case of populations of small-circles and vectors, as proposed by Enkin (1990). This combined average is given in Table 2 and illustrated in Fig. 4(f). It is (in normal polarity): $D_g = 350.0^\circ$, $I_g = 44.6^\circ$ ($k_g = 33.7, \alpha_{95} = 7.8^\circ$) and $D_s = 350.0^\circ$, $I_s = 51.8^\circ$ ($k_s = 94.9, \alpha_{95} = 4.6^\circ$), $n = 12$ sites, in geographic and stratigraphic coordinates, respectively. Here too, the k_s/k_g ratio of 2.816 is higher than the 95 and 99 per cent F values of 2.050 and 2.790, indicating a positive fold test. Indeed, we stress that this assumption of a fairly large relative rotation of Group 2 sites ($44.1^\circ \pm 19.3^\circ$) is quite weak, in particular because we do not have any field observation allowing this to be confirmed. As a consequence the tilt-corrected HTC average can be considered as confidently determined in inclination only, the declination being doubtful. However, interpretations in terms of palaeolatitude of the Torey lakes locality will not be affected by this uncertainty.

Our final discussion on these data concerns the polarity of HTC. As pointed out above, apart from two specimens from site 37, all the resolved HTC directions exhibit reverse polarities. Assuming the HTC are the primary magnetizations of these Early Cretaceous basalts, this may indicate that it has been acquired before the Long Normal Cretaceous superchron, and that the basalts have been emplaced in a relatively short time during a reverse polarity chron. Taking into account the 120 Ma age based on stratigraphic arguments and on early K–Ar dating (Cherbanova & Zvonkova 1966), the single reverse polarity of the data could indicate a slightly older age (around 124 Ma, at the time of the 3-Myr-long M3 reverse magnetic anomaly?). However, a new and precise dating of the basalts is definitely needed to answer this question.

3.2 Siberia block

3.2.1 Early Jurassic Monostoy basalts and trachy-basalts

We thermally demagnetized 56 specimens (Fig. 5) from seven sites of Monostoy basalts and trachy-basalts. Two kinds of behaviour were observed in these samples. A first group (sites 62–66 and 68) exhibited high unblocking temperatures around 600°–680°C, typical of haematite (e.g. specimens 62-482A and 64-497, Fig. 5), whereas the second (sites 61 and 67) demagnetized by 560°C (e.g. specimen 61-477A, Fig. 5), which suggests that magnetite is the carrier of the HTC. The HTC defined in these ranges eventually follows a LTC that is defined in the 0°–200°C temperature range in the first group, and in the 0°–350°C temperature range in the second group. This LTC represents variable amounts from 0 to 90 per cent of the total NRM, and was the dominant magnetization component in samples from sites 61 and 67. At these sites, HTC is poorly defined. Overall, LTC directions are found to be inconsistent, and may be of viscous origin. In the other sites, HTC is generally well defined in the

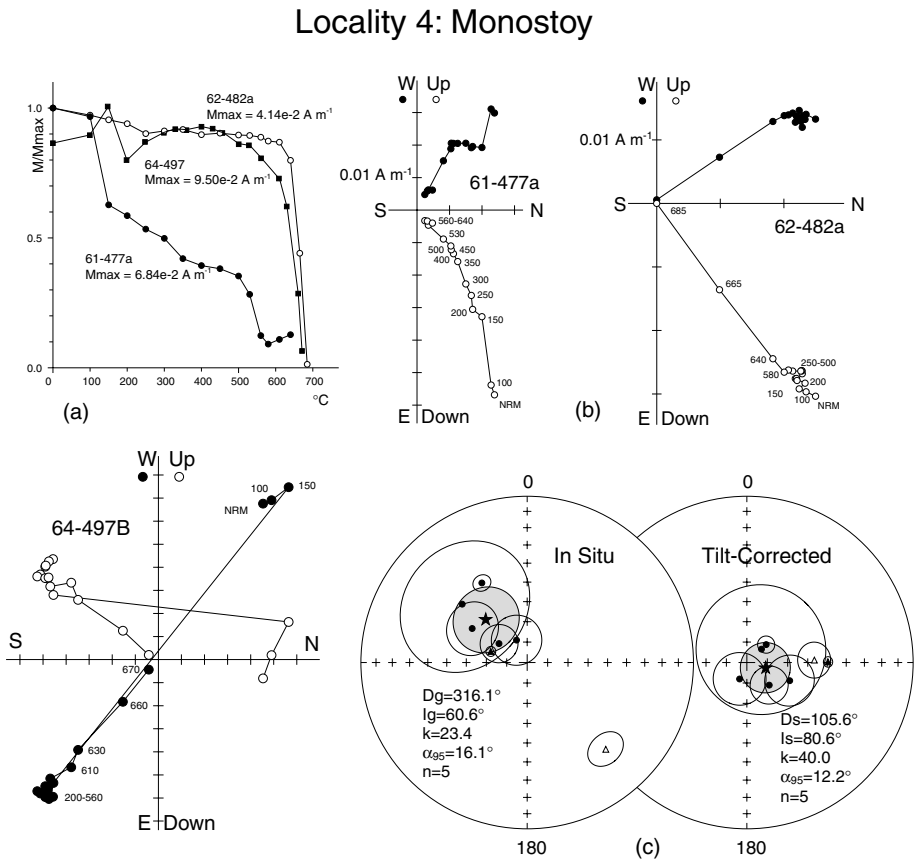

Figure 5. Results of thermal demagnetizations of Monostoy locality samples. (a) Magnetization decay curves. (b) Typical examples of orthogonal vector plots in *in situ* coordinates. Temperatures are indicated in °C. (c) Equal-area projections of HTC site mean directions shown *in situ* (left) and tilt-corrected (right); triangles: sites excluded from the final mean (see text); other conventions as in Fig. 2.

600°–680°C temperature range, and points downward in all sites except site 64.

The site-mean directions of the HTC from sites 61, 62, 63, 66 and 67 are reasonably well grouped (Table 2, Fig. 5c). In contrast, sites 64 and 68 data are clearly divergent. It should be noticed, following field observations, that we have had real difficulties in estimating the flow dips in the field, due to the very poor outcropping conditions of the Monostoy basalts in the Siberian taiga. In particular, the strike of flows 64 and 68 appears anomalous with respect to the other sites (Table 2). For these reasons, we assume that the tilt correction of sites 64 and 68 may be inadequate, and we have excluded them from the final mean for the Monostoy Formation. The HTC directions of the five remaining sites average at $D_g = 316.1°$, $I_g = 60.6°$, $k_g = 23.4, \alpha_{95} = 16.1°$ *in situ* and $D_s = 105.6°$, $I_s = 80.6°$, $k_s = 40.0$, $\alpha_{95} = 12.2°$ after tilt correction (Table 2, Fig. 5c). Both McElhinny (1964) and McFadden (1990) fold tests are inconclusive, which is mainly due to the fact that all the measured flows dip in the same SE direction. However, we note that neither the *in situ*, nor the TC directions conform the present-day dipole field or IGRF directions, and we make the assumption that the TC average HTC direction of Monostoy may represent the Early Jurassic magnetic field in the region.

3.2.2 Early Cretaceous Ingoda river basalts

An IRM acquisition example is presented in Fig. 6(a). It shows that the magnetization increases in fields up to 0.23 T. However, in contrast to the previous examples, no saturation is reached above this value. Instead, the magnetization intensity keeps increasing and does not reach saturation up to a field of 1.2 T. These observations suggest the presence of at least two magnetic minerals with low and high coercivities.

Thermal demagnetization (Figs 6b and c) shows a quite simple behaviour. After a small low-temperature, viscous component removed by 250°C (e.g. specimen 47-364, Fig. 6c), magnetization generally shows a regular decrease, with a stable direction revealing a single HTC of magnetization (Fig. 6c) with systematic north-east downward directions. In most sites, this component is carried by three magnetic minerals (Fig. 6b): a first one which unblocks between 350° and 450°–500°C, a second one which unblocks between 500°C and 580°C and is probably magnetite, and the last one which unblocks between 580° and 650°–680°C and is probably haematite, also responsible for the high coercivity observed in IRM curve (Fig. 6a). Haematite, which generally carries no more than 3–5 per cent of the total NRM, is present in all but sites 39 and 47, where the magnetization is destroyed at 580°C. The demagnetization paths at the specimen level allowed computation of site-mean directions at all sites, but the horizontal flows prevented us from performing a fold test. The between-site mean direction ($D_m = 52.8°$, $I_m = 69.8°, k = 150.5, \alpha_{95} = 3.5°, n = 12$; Table 2) does not contain either the dipolar field direction or the IGRF direction.

3.2.3 Early Cretaceous Bichura basalts and trachy-basalts

Thermal demagnetization of samples from Bichura (Fig. 7) shows a variety of behaviours, as illustrated by the thermal decay curves of

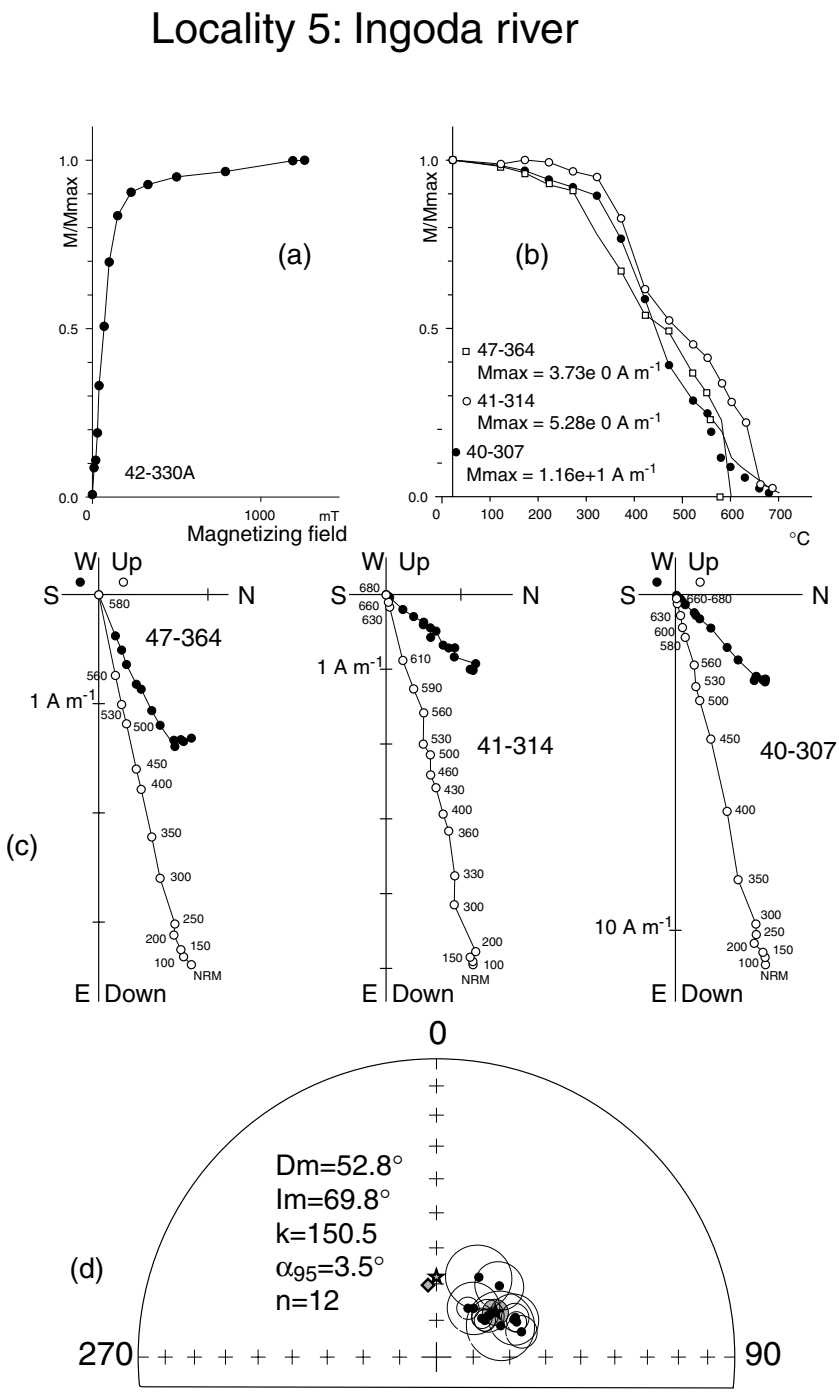

Figure 6. Results of magnetic study of Ingoda river locality samples. (a) IRM acquisition curve showing both low and high saturation field magnetic minerals. (b) Magnetization decay curves. (c) Typical orthogonal vector plot of thermal demagnetizations in *in situ* coordinates. (d) Equal-area projection of *in situ* HTC site-mean directions. There is no tilt correction because of flat-lying flows. Same conventions as in Fig. 2.

Fig. 7(a). The NRM, which ranges between 0.02 and 6.0 A m^{-1}, is completely unblocked by 580°–600°C (specimens 53-412a, 56-438) in some sites, or by 685°C (53-408a, 58-455) in others. This indicates the occurrence of both haematite and magnetite within these samples. The relative contribution of haematite to the total NRM ranges from 0 in sites 52 and 54 to 56, to 100 per cent in sites 57 and 58, and with variable amounts of the order 5–30 per cent in sites 51, 53, 59 and 60. This contribution of haematite may even be variable within single flows, as illustrated by the curves of specimens 53-408a and 53-412a from the same site (Fig. 7a), and there is no clear correlation between this contribution and the average NRM intensity at each site.

Regarding the directions (Fig. 7b), orthogonal vector plots indicate a HTC carried by either haematite (58-455) or magnetite (53-412a, 56-438), or by both (53-408a). In some cases, the HTC could not be precisely determined (e.g. specimen 52-400a), and remagnetization great-circles were used to compute mixed averages at the site level. This HTC was resolved after removing a LTC,

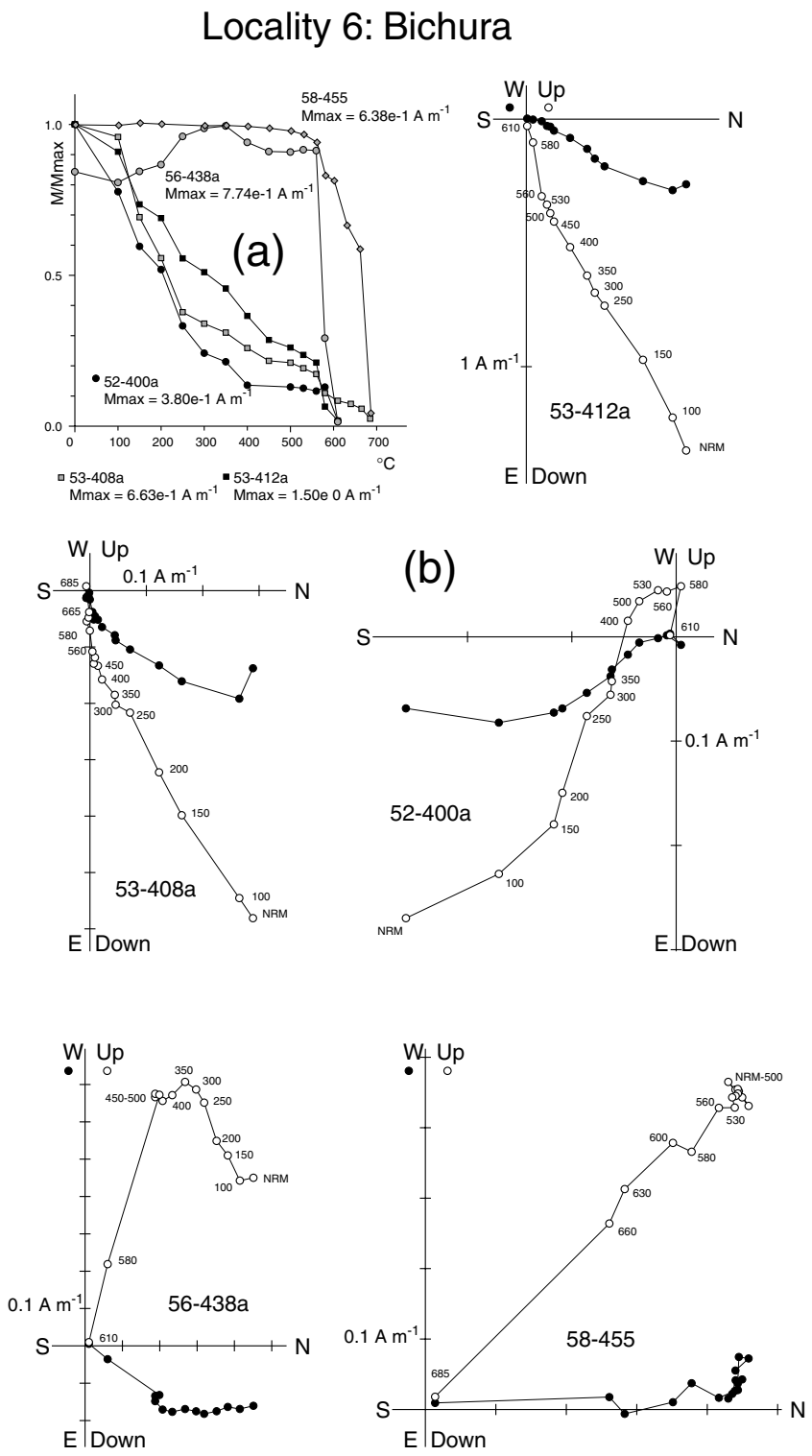

Figure 7. Results of thermal demagnetization of Bichura locality samples. (a) Magnetization decay curves. (b) Typical examples of orthogonal vector plots (*in situ* coordinates). Temperatures are indicated in °C. (c) Equal-area *in situ* projection of specimen LTC. (d) Equal area-projections of site-mean HTC shown *in situ* (left) and tilt-corrected (right); square: site-mean direction of site 51, rejected for the computation of the overall mean direction. Same conventions as in Fig. 2.

which unblocks by 300°–400°C. The LTC was not always observed (e.g. specimen 58-455, Fig. 7b), and was isolated in only 30 specimens out of 66. At the specimen level, the LTC is very scattered (Fig. 7c), but with an obvious tendency to cluster around the present-day dipole field and IGRF directions. The HTC generally shows upward negative inclinations in a north to east direction (e.g. 56-438 and 58-455, Fig. 7b), with the notable exception of site 53 where they have high positive, almost vertical, inclinations. Site-mean

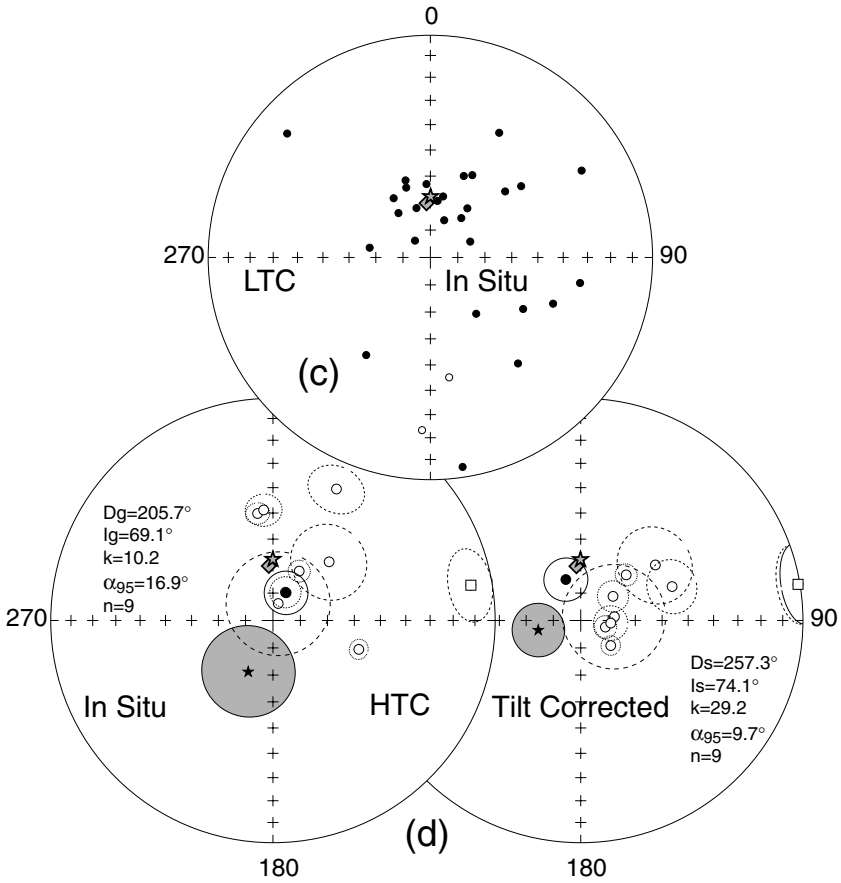

Figure 7. (*Continued.*)

directions are shown in Fig. 7d, *in situ* and after tilt correction. Site 51 shows an anomalous subhorizontal eastward direction and it has been excluded from the final overall mean which averages (in normal polarity) at $D_g = 205.7^\circ$, $I_g = 69.1^\circ$ ($k_g = 10.2, \alpha_{95} = 16.9^\circ$) *in situ*, and $D_s = 257.3^\circ$, $I_s = 74.1^\circ$ ($k_s = 29.2, \alpha_{95} = 9.7^\circ$) $n = 9$ sites, after tilt correction. The tilt correction improves the clustering of data, as illustrated by the reduced α_{95} (Fig. 7d). However, compared to the F statistics at the 95 per cent (2.330) and 99 per cent (3.370) levels, the k_s/k_g ratio of 2.863 indicates a positive fold test at the 95 per cent probability level and an inconclusive one at the 99 per cent level, following McElhinny (1964), and an inconclusive fold test at both levels following McFadden (1990). Altogether, and although it is not very well grouped, we interpret the tilt-corrected HTC as the primary magnetization of Bichura basalts and trachy-basalts.

4 DISCUSSION

Thermal (or composite) demagnetizations allowed us to isolate a stable, high temperature magnetization component (HTC) at each of the 6 localities studied. In most localities, except the Ingoda river locality, this component was separated from a LTC, which, except from Kremljevka peak and Monostoy basalts, conforms to the present-day dipole field axis at the sampling sites and is, therefore, interpreted as a recent overprint. In the Kremljevka peak basalts, the low coercivity/intermediate temperature LTC resolved by composite AF+thermal demagnetizations appeared to have anomalously high intensities, scattered shallow inclinations, and was interpreted as an IRM overprint due to lightning strikes.

Site-mean HTCs display either a single polarity (localities 1, 2, 5), or only one site per locality with a reverse direction (localities 3, 4, 6), preventing us from performing a convincing reversal test. A fold test could be performed only at the Bichura locality (6), where it is positive at the 95 per cent probability level, and inconclusive at the 99 per cent level, and at the Torey lakes locality (3), where it is positive at both levels, but only after assuming that some of the sites have been rotated about vertical axes with respect to the others. In all other localities, because of monoclinal structures and/or flat-lying beds, no fold test could be performed. Altogether, these observations mean that we have no strong stability tests to ascertain the primary origin of resolved HTC in localities 1, 2, 4 and 5. However, because in no case HTC does conform to the present-day (or a recent) dipole field axis in *in situ* coordinates, we make the assumption that we have isolated the primary magnetization at most studied sites. As will be seen in the following discussion, however, the J_3 Unda river Tergen Formation results are not so easily interpreted, and both *in situ* and TC directions will be discussed in more details in that case.

We have computed the palaeopoles from the TC average directions of HTC as given in Table 2, except for the Tergen Formation where we have computed the palaeopoles corresponding to both *in situ* and TC average palaeomagnetic directions. These palaeopoles are listed in Table 3 and illustrated in Figs 8 and 9. In the following, we first discuss the Jurassic, and then the Early Cretaceous results together with other coeval poles available for surrounding Asian blocks, as well as the appropriate parts of the Eurasian Apparent Polar Wander Path (APWP) of Besse & Courtillot (2002), and the NCB APWP of Gilder & Courtillot (1997).

Table 3. Jurassic and Cretaceous palaeopoles from the present study, and surrounding localities from Amuria, Siberia and China blocks.

Block/Area	Formation	Age	Site		Palaeopole				Palaeolatitudes		References
			Lat (°N)	Lon (°E)	Lat (°N)	Lon (°E)	dp/dm (A_{95})	N	Actual (°N)	51°N/112°E (°N)	
Siberia											
Jurassic											
1*(#4)*. Monostoy		J_1	51.1	106.8	43.3	131.4	22.7/23.6	5S	71.7	74.8	This study
2. Ilek	Ilek group	J_{2-3}	56.5	89.5	74.0	135.0	10.4/11.2	101s	65.3	65.1	*Pospelova (1971)*
3. Mogzon	Badin fm.	J_3	51.8	112.0	64.4	161.0	6.7/7.3	9S	62.1	61.6	*Kravchinsky et al. (2001)*
4. Kondersky		$J_3 - K_1$	57.7	134.6	75.0	163.0	10.4/10.9	34s	69.7	58.6	*Pavlov (1993)*
Early Cretaceous											
5*(#5)*. Ingoda river		118–128	51.2	112.2	58.5	176.8	5.2/6.0	12S	53.7	53.4	This study
6*(#6)*. Bichura		110–144	50.6	107.6	37.0	70.4	15.8/17.5	9S	60.3	57.5	This study
Amuria											
Late Jurassic											
7. Unda-Daya	Shadaron fm. *in situ*	J_{2-3}	51.5	117.5	68.6	261.8	3.4/4.9	8S	33.0	31.7	*Kravchinsky et al. (2002)*
	Shadaron fm. TC				59.6	279.0	3.2/5.4	8S	22.1	21.1	*Kravchinsky et al. (2002)*
8*(#1)*. Unda-Daya	Tergen fm. *in situ*	J_3	51.7	117.4	73.3	275.9	5.3/7.4	6S	35.8	34.8	This study
	Tergen fm. TC				58.9	327.3	2.4/4.0	6S	23.2	23.6	”
9. Manzhouli		J_3	47.0	123.1	62.4	224.6	4.9	14S	35.8	35.2	*Zhao et al. (1990)*
10. Hua'an		J_3	49.5	117.5	73.0	254.8	7.8	8S	36.0	36.7	*Zhao et al. (1990)*
Average[(1)]		J_3	50.0	119.0	72.6	262.3	5.2	4L	35.2	—	*see text*
Early Cretaceous											
11.*(#2)*. Kremljevka		125–133	51.8	117.5	86.8	61.8	6.8/7.9	12S	53.5	53.0	This study
12.*(#3)*. Torey lakes		120(?)	50.1	115.9	70.8	322.4	4.3/6.3	12S	32.4	33.7	This study
13. Upper Amur	Taldan fm.	97–146	53.8	124.5	58.3	51.0	3.8/4.6	14s	50.8	55.2	*Halim et al. (1998a)*
14. Chulut Tsagan	Del #12	K	46.1	107.5	86.2	337.5	6.9/8.8	17s	43.6	48.3	*Pruner (1992)*
15. Chulut Tsagan	Del #13	K	46.1	107.5	80.9	12.7	7.7/9.7	19s	44.6	48.7	*Pruner (1992)*
16. Gobi		K	46.1	107.5	72.5	204.5	6.4/8.6	30s	41.4	47.1	*Pruner (1992)*
UCB[(2)]											
United China Block		J_3	—	—	74.9	214.3	6.5	4L	—	—	*Gilder and Courtillot (1997)*
(NCB+SCB)		K_1	*35.0*	*110.0*	78.0	190.2	3.3	9L	—	—	*After Halim et al. (1998a)*

Lat, Lon: Latitude, Longitude of sites and palaeopoles: dp/dm, A_{95}: semi-axes of the confidence ellipse or 95 per cent confidence circle around the palaeopole location, in degrees; N: number of specimens (s), sites (S) or localities (L) used to determine the poles; palaeolatitudes: palaeolatitudes of the actual site locations, and palaeolatitudes of a reference point situated at 51°N, 112°E, on the Mongol-Okhotsk Suture (see Figs 1 and 10). Italic numbers #1 to #6 refer to locality numbers of Fig. 1, Tables 1 and 2. Notes: ([1]) Average J_3 Amuria pole computed after Manzhouli, Hua'an, Shadaron (*in situ*) and Tergen (*in situ*) poles (see text), and attributed to the average location of localities; ([2]) K_1 UCB pole computed after the K_1 NCB and SCB poles listed in Table 2 of Halim *et al.* (1998a), and attributed to an arbitrary reference site in NCB.

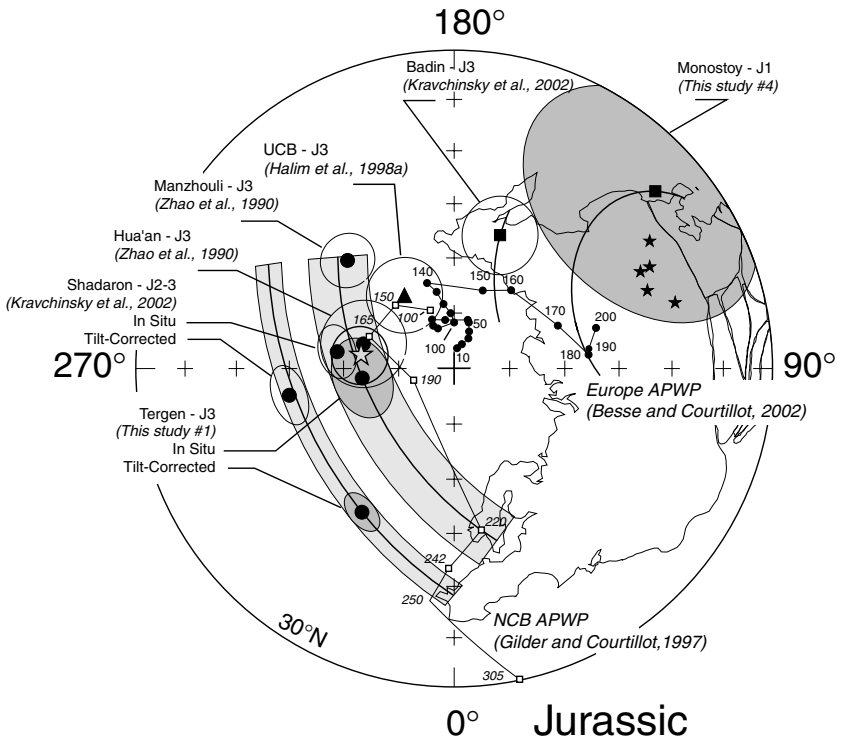

Figure 8. Equal area with selected Jurassic palaeopoles from Amuria (large dots), United China Block (UCB = North + South China Blocks; Halim *et al.* 1998; triangle) and Siberia (squares), with their A_{95} or dp/dm areas of confidence. Dark shaded areas are the poles from the present study: Tergen shown *in situ* (*in situ*) and after tilt correction (TC). Curves passing through Tergen palaeopoles are the small-circles centred on the site locations (small stars). Reference APWP for Europe (small closed dots; Besse & Courtillot 2002) and North China Block (NCB; small open squares; Gilder & Courtillot 1997) are drawn, with ages indicated in Ma. Large grey star with bold circle of confidence: average J_3 palaeopole for Amuria (see text).

4.1 Jurassic

The Early Jurassic Monostoy pole, from north of the Mongol-Okhotsk suture zone (Table 3, Fig. 8), computed after the TC mean direction of Table 2, exhibits a rather large dp/dm ellipse of confidence of 22.7°/23.6°. Although this 188 Ma pole is not located near the Eurasia reference APWP, we note that this discrepancy arises from a clockwise rotation of 119.3° ± 74.0° around the site location with respect to the 190 Ma reference pole, whereas it shows an insignificant palaeolatitudinal movement of 3.5° ± 18.5°. Because of its large uncertainty, firm conclusions cannot be drawn, but we suggest that it may result from tectonic movements along the Mongol-Okhotsk suture, either due to the closure of the Mongol-Okhotsk Ocean, or to the later Tertiary left-lateral shear along the suture as discussed below. It is interesting to note that the path described by our J_1 Monostoy pole, followed by the J_3 Badin pole (Kravchinsky *et al.* 2002) conforms to the reference APWP from ∼190 Ma to ∼140 Ma. Notwithstanding their rather large uncertainties in both position and age, we underline that these two Siberia block palaeopoles are consistent with the Early–Late Jurassic part of the European APWP in terms of palaeolatitude.

Because of the lack of any stability test, we have to consider that the average HTC of the Late Jurassic (J_3) Tergen Formation (Table 2) obtained south of the suture for Amuria block, may be either the primary (pre-tilting) magnetization, or a remagnetization. For this reason, we have computed the palaeopoles from both *in situ* and TC mean HTC (Table 3, Fig. 8). As mentioned above, the Middle–Late Jurassic (J_{2-3}) underlying Shadaron Formation has been studied by Kravchinsky *et al.* (2002) who encountered the same difficulty in choosing between the *in situ* and TC poles as characteristic of the Amuria block. For this reason both *in situ* and TC Shadaron J_{2-3} palaeopoles are drawn in Fig. 8 and given in Table 3. These J_{2-3} and J_3 poles are compared to the J_3 Manzhouli and Hua'an poles obtained by Zhao *et al.* (1990) in Inner Mongolia, which is part of the Amuria block, and to the United China Block (UCB, which is composed of NCB plus SCB) J_3 palaeopole of Gilder & Courtillot (1997).

Our Tergen palaeopole is difficult to interpret. In effect, as is obvious in Fig. 8, the TC pole shows a large discrepancy, in both latitude and declination, with respect not only to the European APWP, but also to the APWP for the NCB, the UCB J_3 pole and, more puzzling, other good quality poles of Zhao *et al.* (1990). This would imply, for example, a northward movement of our sampling area of ∼25° with respect to the UCB since the Late Jurassic, or even more unacceptable, of ∼15° with respect to the Hua'an and Manzhouli palaeopoles (Zhao *et al.* 1990) from the Amuria block itself. Furthermore, compared to the J_{2-3} Shadaron TC pole of Kravchinsky *et al.* (2002), our J_3 Tergen TC pole shows a large counter-clockwise rotation of 26.2° ± 7.3° around the site location, which should have taken place in a rather short time between the emplacement of Shadaron and Tergen effusives, in the Middle–Late Jurassic. In contrast, both poles (Shadaron and Tergen) computed from the *in situ* palaeomagnetic data appear consistent with each other, and with the Amuria palaeopoles of Zhao *et al.* (1990) (Fig. 8).

We, therefore, face a paradoxical situation where our Late Jurassic Tergen effusives (but also the Middle–Late Jurassic Shadaron Formations) would have been remagnetized, after tilting of the formation, in a magnetic field consistent with the Late Jurassic palaeopoles of Amuria, based on the results of Zhao *et al.* (1990). It seems reasonable to exclude a later remagnetization age, because all of the

Cretaceous palaeomagnetic data from UCB (Halim *et al.* 1998a), Amuria (Pruner 1992, and this study) and Siberia (this study) are fully consistent with each other, at least in terms of palaeolatitude differences of sampling areas, as discussed in the next section. If we admit that the Tergen magnetization is indeed a J_3 magnetization, we may consider two possible causes for this anomalous situation. Following one of the possibilities advocated by Kravchinsky *et al.* (2002) for the Shadaron J_{2-3} Formation, one could suggest that the effusives were emplaced after the sedimentary beds were tilted, therefore, implying an erroneous tilt correction. If this explanation is valid for the interbedded andesites, where bedding plane is always difficult to identify in the field, a part of our Tergen collection is made of basalt flows samples, where the tilting could be confidently evaluated in the field. To this, we prefer to recall that, following Zonenshain *et al.* (1990), the Jurassic Formations of Amuria have been folded in Late Jurassic–Early Cretaceous times, in the active tectonics of the Mongol-Okhotsk Ocean closure. We thus propose a scheme where the Middle to Late Jurassic Shadaron and Tergen Formations have suffered an early remagnetization event at the very end of the Jurassic (and/or beginning of the Cretaceous?), most probably because of their proximity to the Mongol-Okhotsk active suture zone. We cannot go further in the estimates of remagnetization age. In effect, both interbedded Shadaron and Tergen effusives are palaeontologically dated, and as cited by Zhao *et al.* (1990), Jurassic effusives from Inner Mongolia show a large range of radiometric ages, from 139 to 199 Ma. Accounting for the above discussion, and the time required to remagnetize the Shadaron and Tergen Formations after the folding, we suggest an older limit at 140–150 Ma for the Manzhouli, Hua'an, Shadaron (*in situ*) and Tergen (*in situ*) palaeopoles.

The last step in the analysis of these J_3 poles is to attempt to compute an average palaeopole for Amuria. As is obvious in Fig. 8, the Shadaron (*in situ*), Tergen (*in situ*) and Hua'an palaeopoles are well grouped, whereas the Manzhouli palaeopole shows a slight clockwise rotation around the site location with respect to this group. We, therefore, allowed this pole to rotate freely around its site location, and computed the average palaeopole position as a mixed average of the small-circle passing through Manzhouli pole and centred on its site location, and the other three (fixed) palaeopoles. The resulting average 140–150 Ma pole for Amuria that we propose lies at (Table 3): $\lambda_p = 72.6^\circ$N, $\phi_p = 262.3^\circ$E ($k = 358.8$, $A_{95} = 5.2^\circ$, $n = 4$), and is shown as a large grey star in Fig. 8. Following the above line of discussion, we consider that this pole could be characteristic for the Late Jurassic of Amuria block. It should be noticed, however, that because of numerous assumptions (e.g. remagnetization of Shadaron and Tergen Formations, rotation of Manzhouli pole, etc.) this pole has a rather tentative position, but we suggest that it may be used for the discussion of palaeolatitudes. Compared to the European reference APWP (Besse & Courtillot 2002), this pole is clearly far sided, as seen from the sampling area. In terms of relative movement between Siberia and Amuria since the Late Jurassic, this difference reflects a significant northward movement with respect to Siberia, of an arbitrary reference point within the Amuria block (50°N, 119°E) of $24.7^\circ \pm 6.7^\circ$, when compared to the 150 Ma pole of the reference APWP, and $15.2^\circ \pm 6.4^\circ$ when compared to the 140 Ma pole. In terms of rotation of Amuria with respect to Siberia, the average Amuria J_3 pole exhibits a slight, perhaps insignificant, counter-clockwise rotation of $-7.1^\circ \pm 14.6^\circ$ to $-12.8^\circ \pm 11.4^\circ$ when compared to the reference APWP poles at 150 and 140 Ma, respectively.

This 1700–2700 km (±700 km) of northward movement of Amuria with respect to Siberia after the Late Jurassic cannot be directly translated in terms of the width of the Mongol-Okhotsk Ocean, because it also depends on the azimuth of the southern Siberia and northern Amuria margins. It would, however, suggest that the ocean was not yet closed by that time, at the longitude of our sampling site. This would contradict the tectonic scheme proposed by Zonenshain *et al.* (1990) who, based on geological arguments, in particular on the occurrence of marine sediments in the collision zone, proposed a Late Triassic–Early Jurassic collision of Amuria in its western part, and a progressively younger closure age toward the east, ending in the Late Jurassic–Early Cretaceous only in the eastern part of the suture. Following these authors, the ocean would have been closed by the Early–Middle Jurassic in the central part of Amuria.

Clearly, the J_{2-3} database from palaeomagnetism is not yet sufficient to solve the remaining structural and palaeogeographic debates in this area. We note that there is some (weak and conflicting, but interesting) suggestions from our palaeomagnetic results that Amuria had not yet amalgamated to Siberia by the end of the Jurassic. Only new palaeomagnetic investigations in this region will help to solve the remaining uncertainties on the exact palaeoposition of the blocks composing this part of the Asian mosaic.

4.2 Early Cretaceous

The Early Cretaceous poles (Table 3) for the Ingoda River and Bichura localities from the Siberia block and for the Kremljevka Peak and Torey Lakes localities from the Amuria block are shown in Fig. 9, where they are compared to the Early Cretaceous Taldan (Amur province) pole of Halim *et al.* (1998a) and three Cretaceous poles (Gobi, Chulut Tsagan Del #12 and #13) of Pruner (1992) from the Amuria block. From the Cretaceous poles of the North and South China blocks listed by Halim *et al.* (1998a) we have recomputed an average pole for UCB limited to the Early Cretaceous. This pole (Table 3) lies at 76.3°N, 203.2°E, $A_{95} = 3.5^\circ$ ($k = 211.3$, $n = 9$).

It is clear from Fig. 9, that these poles are widely scattered. If we select only the poles of (proven or suspected) Early Cretaceous age (K_1), excluding the Torey lakes palaeopole that is discussed below, we observe that four palaeopoles coming from either side of the Mongol-Okhotsk suture (Ingoda and Bichura from the north, Kremljevka peak and Taldan from the south) align remarkably well on a small-circle centred on the average site location (52.0°N, 115.3°E), defined with a confidence limit of ±1.4° (darker shaded zone in Fig. 9), and which contains the 100, 110 and 120 Ma poles of the European reference curve (Besse & Courtillot 2002). We notice that the less well defined, in terms of age, Amuria Cretaceous palaeopoles of Pruner (1992) also align on a small-circle centred on site position (light shaded zone in Fig. 9), with a larger zone of confidence (±4.0°) which, however, covers the whole Cretaceous part of the reference European APWP and overlaps our K_1 small-circle.

This alignment of K_1 palaeopoles from the Trans-Baikal area along a common small-circle leads to two major conclusions:

(1) there has been no relative north–south movement of Amuria versus Siberia block localities since the Early Cretaceous. This supports the hypothesis that the Mongol-Okhotsk Ocean was closed by that time. We can tentatively estimate the time of closure more precisely. According to the stratigraphic K_1 age of Taldan (Halim *et al.* 1998a), to the radiometric ages of Ingoda and Kremljevka effusives (118–128 Ma and 125–135 Ma, respectively), and to the lack of reversed polarity within these localities (with the exception of the Bichura pole, which comes from mostly reverse magnetizations, and could have an earlier age), these formations could have

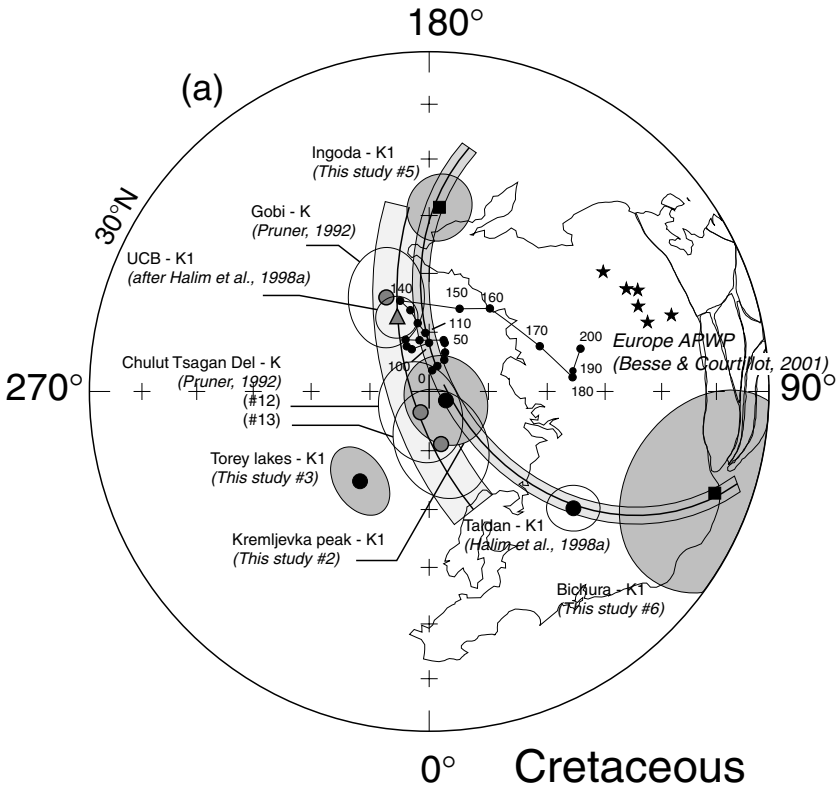

Figure 9. Equal area projection with selected Early Cretaceous and Cretaceous palaeopoles from Amuria (circles), UCB (triangle) and Siberia (squares), with their A_{95} or dp/dm areas of confidence. Dark shaded areas are the poles from the present study: Ingoda and Bichura localities from Siberia, and Torey lakes and Kremljevka peak localities from Amuria. Two small-circles centred on the average site locations are drawn: one (very light shading) passing through the Cretaceous palaeopoles of Pruner (1992), the second (light shading) passing through the Early Cretaceous poles of Siberia and Amuria, excluding Torey lakes pole. Other conventions and Europe APWP as in Fig. 8.

been emplaced in the beginning of the Cretaceous Long Normal Superchron at about 100–120 Ma.

(2) The alignment of palaeopoles along a small-circle demonstrates the large clockwise or counter-clockwise post-Early Cretaceous rotations affecting the sampling areas. With respect to the 110 Ma reference pole (80.0°N, 183.6°E, $A_{95} = 4.2°$), these rotations amount to $-20.4° \pm 15.2°$ (counter-clockwise) for Kremljevka peak, $-69.1° \pm 10.7°$ (counter-clockwise) for Taldan, $+36.7° \pm 12.3°$ (clockwise) for Ingoda river and $-118.7° \pm 36.0°$ (counter-clockwise) for Bichura. We have also roughly estimated the rotations of the Gobi desert palaeopoles of Pruner (1992) with respect to the average Cretaceous European palaeopole (average of the 70–140 Ma reference palaeopoles: 79.3°N, 194.4°E, $A_{95} = 2.4°$, $n = 8$), which amount to $8.1° \pm 12.0°$ (clockwise) for Gobi locality, $-19.4° \pm 12.6°$ (counter-clockwise) for Chulut Tsagan Del #12 and $-28.2° \pm 14.1°$ (counter-clockwise) for Chulut Tsagan Del #13.

The interpretation of these rotations is not straightforward. However, we make the following observations. First, the great variability of these rotations, which range from clockwise 37° (Ingoda river) to counter-clockwise $-120°$ (Bichura), demonstrates that they do not reflect a bulk rotation of the Trans-Baikal region with respect to stable Europe. Rather, it suggests that they are rotations of the sampled areas around local vertical axes, which might be due to a post-Cretaceous heterogeneous deformation of the continental crust in the vicinity of the Mongol-Okhotsk suture. Second, we note that, apart from the insignificant rotation of the Gobi pole and the clockwise (anomalous?) rotation of the Ingoda river locality, all the other poles are rotated counter-clockwise, whether they come from Siberia or Amuria blocks. Altogether, these observations are consistent with the hypothesis of Halim *et al.* (1998b) of the existence of a major post-Cretaceous sinistral shear zone separating Siberia from the southern regions of Asia, and accommodating the eastward extrusion of Amuria, NCB and SCB during the Tertiary, under the effect of India penetrating into Eurasia. This major shear zone, with a probable transpressive component, which could be responsible for the anomalous sense of rotation of Ingoda river region, was initially postulated by Halim *et al.* (1998b) as being located on the Mongol-Okhotsk suture, but our new data, together with the previous results of Pruner (1992) and Halim *et al.* (1998a), suggest that it could involve a larger crustal area, covering the whole Trans-Baikal and northern Mongolia regions.

We now turn to the anomalous position of the Torey Lakes palaeopole (Table 3, Fig. 9), which shows a discrepancy with all of the other Early Cretaceous poles of the region. The Torey lakes basalts are supposed to be 120 Ma old, based on stratigraphic arguments and an early K–Ar date (Cherbanova & Zvonkova 1966). We may invoke two hypotheses, both based on age uncertainties. First, if the age is indeed correct, the palaeopole position would indicate a post-Early Cretaceous northward movement of the Torey area of $19.6° \pm 3.9°$ with respect to the 120 Ma Eurasian reference pole (and a counter-clockwise rotation of $-28.6° \pm 8.4°$). The same amount of northward movement would have occurred also with respect to Kremljevka peak and Taldan localities from the Amuria block, which does not seem reasonable. A second, and, in our opinion, more conceivable hypothesis would be a slightly older age for

these basalts. In effect, if these basalts are a little older by, say, 20–30 Ma, and recalling the rapid closure of the Mongol-Okhotsk Ocean as discussed above, the palaeopole here obtained would be consistent with the Late Jurassic poles and thus could constrain the closure of the ocean at the Late Jurassic–Early Cretaceous boundary. In any case, only new and precise dating of these basalts could answer this question.

5 CONCLUSIONS

We have presented a palaeomagnetic study of six localities of Jurassic and Early Cretaceous effusives from both sides of the Mesozoic Mongol-Okhotsk suture, which cuts the Trans-Baikal region of South Siberia, separating the Siberia block to the north from the Amuria block to the south. This suture represents the northern block limit of the tectonic system comprising the Asian mosaic. Our objective was to answer two main questions:

(1) can the Jurassic closure of the Mongol-Okhotsk suture, as proposed by Zonenshain *et al.* (1990), be confirmed and made more precise;

(2) what is the role of this boundary in the Tertiary tectonic evolution of the Asian mosaic (Chen *et al.* 1993; Halim *et al.* 1998b) as India indents into Asia? To these two questions, despite difficulties due to often poor outcropping conditions in these remote areas, and to somewhat complicated palaeomagnetic results, our new data may contribute some answers.

For Jurassic times, our Monostoy J_1 pole from the Siberia block, although rotated about a local vertical axis, is consistent in palaeolatitude with the Early Jurassic part of the European APWP. In contrast, the Tergen J_3 pole from the Amuria block is discordant with this APWP. However, it agrees with the J_{2-3} Shadaron pole of Kravchinsky *et al.* (2002) obtained in the same region, and the J_3 Manzhouli and Hua'an poles of Zhao *et al.* (1990) from Inner Mongolia. Altogether, these poles suggest that the Mongol-Okhotsk Ocean was still open at the end of the Jurassic. This result conflicts with the interpretation of Zonenshain *et al.* (1990) who proposed a Middle Jurassic closure. Turning to Early Cretaceous times, our data from both sides of the suture, although quite scattered, but aligning on a common small-circle, indicate that the accretion of Amuria to Siberia was achieved by that time. The evolution of this closure is illustrated in Fig. 10 where we have drawn palaeolatitude as a function of time for a reference point currently situated at 51°N 112°E (Table 2) on the suture itself (see Fig. 1). This Fig. suggests that the intervening ocean was widely opened in Late Jurassic time ($\Delta\lambda = 26.8° \pm 6.8°$ between points 3 and 8 in Fig. 10), and closed by the Early Cretaceous. This means that the Mongol-Okhotsk Ocean closed rapidly with plate velocities on the order of $\sim$15 cm yr^{-1}. This conclusion is now based for the first time on palaeomagnetic data coming from both the Siberia and Amuria blocks, in the vicinity of the Mongol-Okhotsk suture itself.

The broad small-circle distribution of Cretaceous palaeopoles indicates that the Trans-Baikal area has suffered significant post-Cretaceous heterogeneous deformation marked by variable amounts of rotation of the sampled sites around local vertical axes. These rotations are almost all counter-clockwise, with the exception of the anomalous clockwise rotation of the Ingoda river locality in Siberia (locality 5, Fig. 1). This supports the idea that the Mongol-Okhotsk suture, or more generally the Trans-Baikal area, acts as a transpressive sinistral megashear, as proposed by Halim et al. (1998b), allowing eastward extrusion of Amuria and the NCB and NCB in the Tertiary, due to the penetration of India into Eurasia.

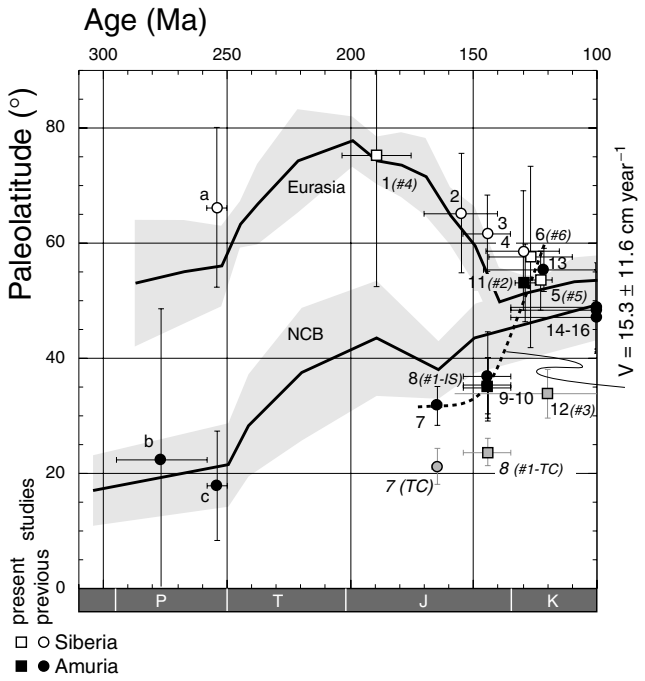

Figure 10. Palaeolatitude versus time for a reference point situated at 51°N 112°E, on the Mongol-Okhotsk geosuture (see R in Fig. 1). The European and NCB APWP's are shown as continuous lines with shaded areas of confidence. Points labelled a, b and c are computed from the Permian poles of Kravchinsky *et al.* (2002). Numbers 1–16 refer to poles listed in Table 3, labels #1 to #6 in italics between brackets refer to locality numbers of the present study (Fig. 1); closed (open) symbols: palaeolatitudes computed from poles from Amuria (Siberia); squares (circles): present (previous) studies; grey symbols: points of lower reliability as discussed in text; dotted line represents the closure of the Mongol-Okhotsk Ocean, between {8–10} and {4–6, 11 and 13} groups of points, at a rate of 15.3 ± 11.6 cm yr^{-1}.

This indicates that this neglected block boundary probably plays a major role in the Tertiary tectonics of Asia.

Finally, although our new data bring useful insights into Asian late Mesozoic and Tertiary tectonics, we feel that further investigations are needed, in particular to get palaeomagnetic data with better stability tests, obtained on well-dated formations. The problem of dating is crucial, because of the contradictions that exist between the geological and palaeomagnetic estimates of the time of closure of the Mongol-Okhotsk Ocean.

ACKNOWLEDGMENTS

This work was conducted in the frame of a cooperation project between IPGP and the Irkutsk Institute of Geochemistry, Siberian Branch of the Russian Academy of Sciences (SBRAS), supported by the European INTAS project No 94-1253. We thank Mrs L. Starukhina and Mr V. Asoskov from Chita Geological Service for efficient organization, guidance and help in the 1997 field expedition to Trans-Baikal. V. Ivanov, from the Irkutsk Institute of Geochemistry of SBRAS, helped us and supplied maps of outcrops in Siberia and Mongolia. An early version of this paper benefited from comments and constructive criticisms made by T. Rolf, R. Van der Voo, J. Geissman, F. Heller, Y. Otofuji and an anonymous reviewer. We also thank V. Courtillot and S. Gilder for thoughtful comments on this article. This final version was carefully reviewed by R. Van der Voo and C. Mac Niocaill. This is contribution No 2082 of IPGP.

REFERENCES

Besse, J. & Courtillot, V., 2002. Apparent and true polar wander and the geometry of the geomagnetic field in the last 200 million years, *J. geophys. Res.,* **107,** 1–31.

Chen, Y., Courtillot, V., Cogné, J.-P., Besse, J., Yang, Z. & Enkin, R., 1993. The configuration of Asia prior to the collision of India: cretaceous paleomagnetic constraints, *J. geophys. Res.,* **98,** 21 927–21 941.

Cherbanova, L.F. & Zvonkova, M.B., 1966. Geological composition and mineral resources of Torey lakes region. Report after 1964-1965 years work of Casuchevsky geological team (scale 1:200000). Chita Geological Company, p. 278, (in Russian).

Cogné, J.P. , 2003. PaleoMac: a Macintosh™ application for treating paleomagnetic data and making plate reconstructions, *Geochem. Geophys. Geosyst.,* **4**(1), 1007, doi:10.1029/2001GC000227.

Enkin, R., 1990. Formation et déformation de l'Asie depuis la fin de l'ère primaire, *PhD thesis*, IPG, Paris.

Enkin, R., Courtillot, V., Xing, L., Zhang, Z., Zhuang, Z. & Zhang, J., 1991. The stationary Cretaceous paleomagnetic poles of Sichuan (South China Block), *Tectonics,* **10,** 547–559.

Enkin, R., Yang, Z.Y., Chen, Y. & Courtillot, V., 1992. Paleomagnetic constraints on the geodynamic history of China from the Permian to the Present, *J. geophys. Res.,* **97,** 13 953–13 989.

Fisher, R.A., 1953. Dispersion on a sphere, *Proc. R. Soc. London,* **217,** 295–305.

Gilder, S. & Courtillot, V., 1997. Timing of the North-South China Collision from New Middle to Late Mesozoic Paleomagnetic Data from the North China Block, *J. geophys. Res.,* **102,** 17 713–17 727.

Gilder, S.A., Zhao, X.X., Coe, R.S., Wu, H.R. & Kuang, G.D., 1993. Discordance of Jurassic paleomagnetic data from South China and their tectonic implications, *Earth planet. Sci. Lett.,* **119,** 259–269.

Gilder, S.A., Zhao, X., Coe, R.S., Meng, Z., Courtillot, V. & Besse, J., 1996. Paleomagnetism and Tectonics of the Southern Tarim Basin, Northwestern China, *J. geophys. Res.,* **101,** 22 015–22 031.

Halim, N., Kravchinsky, V., Gilder, S., Cogné, J.P., Alexyutin, M., Sorokin, A. & Courtillot, V., 1998a. A Paleomagnetic study from the Mongol-Okhotsk Region: Rotated Early Cretaceous Volcanics and Remagnetized Mesozoic Sediments, *Earth planet. Sci. Lett.,* **159,** 133–146.

Halim, N. et al, 1998b. New Cretaceous and Lower Tertiary paleomagnetic results from Xining-Lanzhou basin, Kunlun and Qiangtang blocks, China: implications on the Geodynamic evolution of Asia, *J. geophys. Res.,* **103,** 21 025–21 046.

Halls H.C., 1978. The use of converging remagnetization circles in palaeomagnetism, *Phys. Earth planet. Int.,* **16,** 1–11.

Huang, K. & Opdyke, N.D., 1991. Paleomagnetism of Jurassic rocks from southwestern Sichuan and the timing of the closure of the Qinling suture, *Tectonophysics,* **200,** 299–316.

Kazimirovsky M.E., 1994. Space-time and compositional evolution of magmatism of Nercha-Ingoda rift zone (Trans-Baikalia). *Russian Geology and Geophysics,* **N3,** 40–49.

Kazimirovsky, M.E. & Drill, S.I., 1991. Compositional features and genesis of lower Cretaceous rift effusives of Chita-Ingoda depression (Central Trans-Baikalia), *Doklady Academii Nauk USSR,* N5, v.321, 1062–1065.

Kirschvink, J.L., 1980. The least squares line and plane and the analysis of the paleomagnetic data, *Geophys.J. R. astr. Soc.,* **62,** 699–718.

Kravchinsky, V.A., 1995. Paleomagnetic study in Mongol-Okhotsk folded belt, *PhD thesis*, Irkutsk State Technical University, Irkutsk, (in Russian).

Kravchinsky, V.A., Cogné, J.-P., Harbert, W. & Kuzmin, M.I., 2002. Evolution of the Mongol-Okhotsk ocean with paleomagnetic data from the suture zone, *Geophys. J. Int.,* **148,** 34–57.

Kuzmin, M.I., 1985. *Geochemistry of magmatic rocks of Phanerozoic Mobil Fold Belts*, Nauka, Novosibirsk, (in Russian).

Kuzmin, M.I. & Filippova, I.B., 1979. History of Mongol-Okhotsk folded belt development in Middle-Late Palaeozoic and Mesozoic, in *Structure of Lithosphere Plates,* Inst. Oceanology Publ. House, Moscow, pp. 189–226.

Kuzmin, M.I. & Kravchinsky, V.A., 1996. First paleomagnetic data on the Okhotsk-Mongolian belt, *Russian Geology and Geophysics,* **37,** 48–55.

Lin, J.L., Fuller, M. & Zhang, W.Y., 1985. Preliminary Phanerozoic polar wander paths for the North and South China blocks, *Nature,* **313,** 444–449.

McElhinny, M.W., 1964. Statistical significance of the fold test in paleomagnetism, *Geophys. J. R. astr. Soc.,* **8,** 33–40.

McFadden, P.L., 1990. A new fold test for paleomagnetic studies, *Geophys. J. Int.,* **103,** 163–169.

McFadden, P.L. & Reid, A.B., 1982. Analysis of paleomagnetic inclination data, *Geophys. J. R. astr. Soc.,* **69,** 307–319.

McFadden, P.L., Merill, R.T., McElhinny, M.W. & Lee, S., 1991. Reversal of the Earth's magnetic field and temporal variations of the dynamo families, *J. geophys. Res.,* **96,** 3923–3933.

McFadden, P.L. & McElhinny, M.W., 1988. The combined analysis of remagnetization circles and direct observations in paleomagnetism, *Earth planet. Science Letters,* **87,** 152–160.

Misnik, Y.V. & Shevchuk, V.V., 1980. Eastern Trans-Baikal ancient block and its role for forming of regional structure, *Geotectonica,* **5,** 25–37.

Nie, S., 1991. Paleoclimatic and paleomagnetic constraints on the Paleozoic reconstructions of South China, North China and Tarim, *Tectonophysics,* **196,** 279–308.

Parfenov, L.M., 1984. *Continental margins and island arcs of Mesozoids of North-Western Asia*, Nauka, Novosibirsk, (in Russian).

Pavlov, V.E., 1993. Paleomagnetic directions and paleomagnetic pole positions: Data for the former USSR, Issue 8, VNIGRI Institute, St. Petersburg, (unpublished Catalogue).

Pospelova, G.A., 1971. Paleomagnetic directions and pole positions: Data for the USSR, Issue 1, Soviet Geophysical Committee: World Data Center-B (Moscow), catalogue.

Pruner, P., 1992. Paleomagnetism and paleogeography of Mongolia in the Cretaceous, Permian and Carboniferous—final report, *Phys. Earth planet. Int.,* **70,** 169–177.

Tapponnier, P., Peltzer, G. & Armijo, R., 1986. On the mechanics of the collision between India and Asia, *Geol. Soc. Spec. Publ. London,* **19,** 115–157.

Thomas, J.C., Perroud, H., Cobbold, P.R., Bazhenov, M.L., Burtman, V.S., Chauvin, A. & Sadybokasov, E., 1993. A paleomagnetic study of Tertiary formations from the Kirgiz Tien Shan and its tectonic implications, *J. geophys. Res.,* **98,** 9571–9589.

Sinitsa, S.M. & Starukhina, L.P., 1986. New data and problems of stratigraphy and paleontology of Upper Mesozoic of Trans-Baikal region, in *New data on Trans-Baikal Geology*, Chita, Geological State Company, pp. 46–51, 1986, (in Russian).

Skoblo, V.M. & Lyamina, N.A., 1985. Irkutsk basin. Western and Eastern Trans-Baikalia, in *Jurassic Continental Biosenoses of South Siberia and Surrounded Territories*. Publ. House 'Nauka', Moscow, pp. 41–56, (in Russian).

Shubkin, S.P., Beljakov, E.A. & Beljakov, I.P., 1992. Geology and mineral resources of Unda and Kurenga rivers basins. Report of Shivija team about results of geological investigations of scale 1:50000 during 1987–1991 years in Unda-Daya polygon, *Publishing of Geological company 'Chita-geologija'*, p. 672, Vol. 1, (in Russian).

Sorokin, A.A., 1992. Geochemistry and geodynamic position of magmatic rocks of the central segment of the Mongol-Okhotsk fold belt, *PhD thesis*, Institute of Geochemistry, Siberian Branch of the Russian Academy of Science, Irkutsk, (in Russian).

Srebrodol'skaya, I.N., 1984. New data about late Jurassic flora of Trans-Baikalia. Matherials about stratigraphy and paleogeography of Eastern Asia (new data). Vladivostok, Academy of sciences of the USSR, pp. 40–47 (in Russian).

Xu, X., Harbert, W., Drill, S. & Kravchinsky, V., 1997. New paleomagnetic data from the Mongol-Okhotsk collision zone, Chita region, south central Russia: implications for Paleozoic paleogeography of the Mongol-Okhotsk ocean, *Tectonophysics,* **269,** 113–129.

Yang, Z. & Besse, J., 2001. New Mesozoic apparent polar wander path for south China: tectonic consequences, *J. geophys. Res.,* **106,** 8493–8520.

Yang, Z., Courtillot, V., Besse, J., Ma, X., Xing, L. & Zhang, J., 1992. Jurassic paleomagnetic constraints on the collision of the north and South China blocks, *Geophys. Res. Lett.,* **19,** 577–580.

Yarmoljuk, V.V., Vorontsov, A.A., Ivanov, V.G., Kovalenko, V.I., Baikin, D.N. & Sandimirova, G.P., 2000. Stages of bimodal and alkaline-granite

magmatism in the western Transbaikalia (geochronological data on the Tugnui depression), *Reports of the Russian Academy of Sciences,* **373,** 78–86.

Zhao, X. & Coe, R.S., 1987. Paleomagnetic constraints on the collision and rotation of North and South China, *Nature,* **327,** 141–144.

Zhao, X., Coe, R.S., Zhou, Y., wu, H. & Wang, J., 1990. New paleomagnetic results from northern China: collision and suturing with Siberia and Kazakstan, *Tectonophysics,* **181,** 43–81.

Zijderveld, J.D.A., 1967. Demagnetization of rocks: analysis of results, in *Methods in Paleomagnetism*, Collinson, D.W., Creer, K.M. & Runcorn, S.K., eds, pp. 254–286, Elsevier, Amsterdam.

Zonenshain, L.P. & Kuzmin, M.I., 1997. *Paleogeodynamics*, Am. geophys. Un., Washington.

Zonenshain, L.P., Kuzmin, M.I. & Moralev, V.M., 1976. *Global Tectonics, Magmatism and Metallogeny*, Nedra, Moscow, (in Russian).

Zonenshain, L.P., Kuzmin, M.I. & Natapov, L.M., 1990. Geology of the USSR: A Plate Tectonic Synthesis, *Geodynamics Series 21*, AGU, Washington, DC, p. 242.